A Mathematical Model of the Bag-Cell Neuron in Aplysia Californica

by

Drew Lloyd

A thesis
presented to the University of Waterloo
in fulfillment of the
thesis requirement for the degree of
Master of Mathematics
in
Applied Mathematics

Waterloo, Ontario, Canada, 2011

I hereby declare that I am the sole author of this thesis. This is a true copy of the thesis, including any required final revisions, as accepted by my examiners.

I understand that my thesis may be made electronically available to the public.

Abstract

Aplysia Californica are marine mollusks with a relatively simple central nervous system that makes them ideal for investigating neurons. The bag-cell neuron is found in the Aplysia and is important due to its activity causing the onset of a series of behaviours which culminate in egg laying. The bag-cell neuron is generally not very active but can be stimulated into a long active period known as the afterdischarge in which the neuron releases a hormone that causes egg laying. The afterdischarge is due to a fundamental change in the electrophysiological properties of the bag-cell neuron. The purpose of this thesis is to determine a mathematical model for the electrical activity found in a single bag-cell neuron which can be used to investigate the afterdischarge behaviour.

Acknowledgements

Table of Contents

List of Tables

List of Figures

Chapter 1

Introduction

Aplysia Californica are marine mollusks with a relatively simple central nervous system that makes them ideal for investigating neurons. This is because the neural activity in an Aplysia directly links to the animal's behaviour. The bag-cell neuron is a neuron found in the Aplysia whose activity causes the onset of a series of behaviours which culminate in egg laying. This happens due to two clusters of 200-400 bag-cells activating synchronously and releasing a hormone which will cause the animal to initiate egg laying behaviour. The synchronous activation is a specific kind of neuronal activity known as the afterdischarge in which a brief amount of stimulation causes the cell to be very active for up to several hours during which the egg laying hormone is released. The purpose of this thesis is to determine a mathematical model for the electrical activity found in a single bag-cell neuron which can be used to investigate the afterdischarge behaviour.

1.1   Outline of Thesis

In Chapter 2 we will review the biology and function of neurons. We will follow this with a review of the principles and mathematics involved in modelling the electrophysiology of neurons by looking at the Nobel prize winning work done by Hodgkin and Huxley in the late 1940's and early 1950's. Specifically we will be discussing what it means for a cell to be excitable and how the relevant properties of neurons can be measured so that a mathematical model of the behaviour can be created. We will then review the original model created by Hodgkin and Huxley of a squid giant axon. In Chapter 3 we will discuss the biology and physiology of Aplysia and its bag-cell neuron. We will then look at the literature regarding bag-cell neurons from which we develop our model. In Chapter 4 we will go through the steps of building the model of the bag-cell neuron and discuss the results and limitations as well a further work that can be done to improve the model. Finally in Chapter 5 we will review the results from the model we created and discuss its limitations and future work which can be done to improve the model.

Chapter 2

Neurobiology Background

2.1 Neurons

It has been known since the 19th century that cells are the basic elements of living organisms. Neurons are the building blocks of a central nervous system. They are electrically excitable cells that are responsible for transmitting information using electrical or chemical signals. Neurons have an incredible range of distinct cell types that allow them to have different functions.

Neurons have the same basic cellular structure as other cells, i.e. a cell body containing a nucleus, endoplasmic reticulum, ribosomes, Golgi apparatus, mitochondria and other organelles. The important differences between neurons and other cells comes from two structures: the dendrites and the axon. The dendrites form a tree like structure ("dendron" is Greek for tree) arising from the cell body which receives inputs from other neurons (the dendritic arbor). The number of inputs a neuron receives is dependent on the complexity of its dendritic arbor. The axon is a unique extension of the neuronal cell body that extends from a few μm to significantly longer depending on the specific cell and its function. For example, the sciatic nerve in humans has an axon which extends from the base of the spine to the big toe. The point where the axon is connected to the cell body or soma is called the axon hillock and the point at which the axon ends is called the terminal button. At the terminal button there are vesicles, small membrane enclosed sacks, which can release chemicals (neurotransmitters) into a small gap between the end of the axon and the dendrite of the adjacent cell. A labelled neuron is shown in Figure 2.1

The fundamental characteristic of a neuron is its ability to generate electrical signals that transmit information. Even though neurons are not good conductors of electricity, they have developed elaborate mechanisms for generating electrical signals using the flow of ions across their cell membranes. The electrical signal is an all-or-nothing event known as an action potential. Action potentials are transient depolarizations (changes in membrane potential in the positive direction) in the electrical potential of the cell membrane. Action potentials
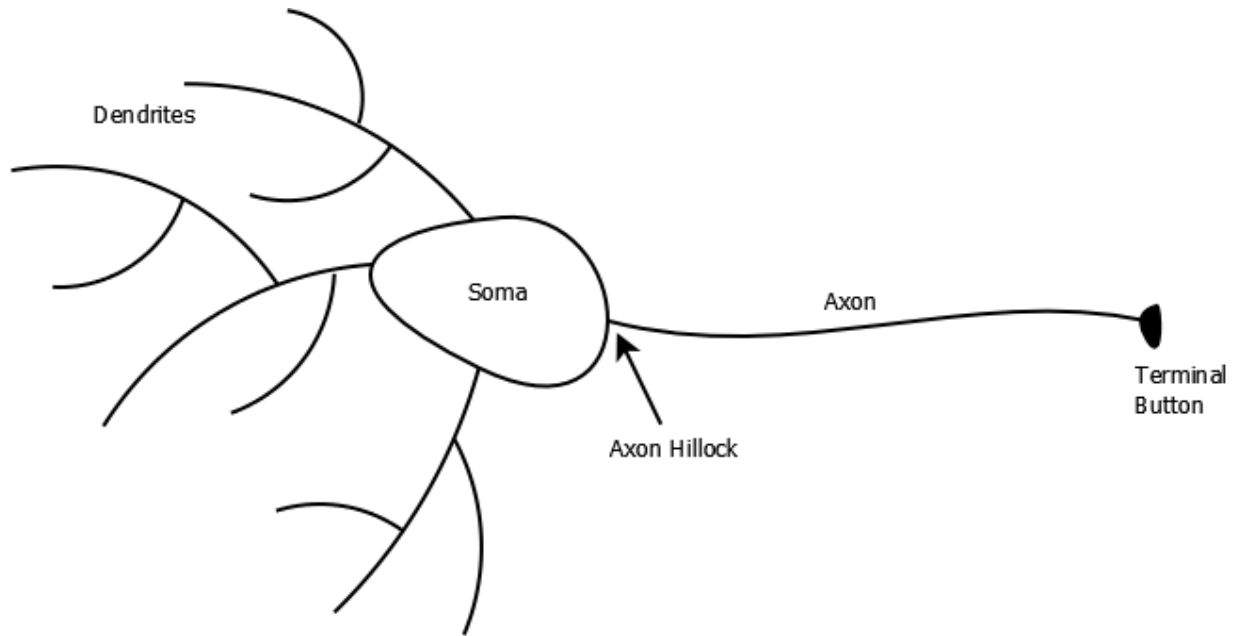
Figure 2.1: A typical Neuron

are also known as "spikes" or "impulses". An all-or-nothing event refers to the property of the spike that the amplitude is the same regardless of the amount of stimulation as long as it is above a certain threshold value. The signal is transmitted through a neuron starting at the dendrites. The dendrites receive signals from other neurons, increasing the membrane potential where the signal is received. This change spreads passively along the membrane to the axon hillock. Passive spread refers to the spread of a change in membrane potential where a local membrane depolarization causes the area around the initial depolarization to also become depolarized slightly. The amount of depolarization in the membrane decreases exponentially with distance from the initial site. If the membrane potential at the axon hillock reaches a certain threshold value then an action potential is initiated that travels down the axon to the terminal button where the signal is then transmitted to other neurons. The place where the axon of one cell and the dendrite of the cell it is communicating with are nearest is known as the synapse and the gap between the two is known as the synaptic cleft. The cell sending a signal is called the efferent cell and the receiving cell is called the afferent cell.

The transmission of a signal between two cells through the synapse consists of the following: the signal starts at the axon hillock of a neuron and travels down the axon to the terminal button, at the terminal button neurotransmitters are released into the space between the efferent neuron's axon and the afferent neuron's dendrite, the neurotransmitters bind to sites on the dendrite of the afferent cell and cause the signal sent by the efferent neuron to propagate through the dendrites to the axon hillock of the afferent neuron. Specifically the neurotransmitters cause protein channels to open allowing ions in. This produces

3

a positive change in the membrane potential of the dendrites which spreads. Eventually the spreading depolarization reaches the axon hillock and since the difference in membrane potential typically decays exponentially with distance from the synapse and time, it often takes several efferent neurons' inputs to stimulate an action potential.

Another way for action potentials to propagate from neuron to neuron is by gap junctions. Gap junctions occur where two neurons are so close together that their cytoplasms are directly connected by groups of proteins called connexons which extend from each cell to bridge the extracellular space. This allows for ions to freely flow from one cell to another. This means that if one cell membrane becomes very depolarized, the depolarization will spread to the other cell.

2.2   Electrophysiology

The main focus of the mathematical model presented in Chapter 4 is to build a model that describes and provides insight into the understanding of the action potential in a bag-cell neuron. In order to understand an action potential in a bag-cell neuron we will first examine the seminal work by Hodgkin and Huxley. In the late 1940's and early 1950's they formulated a model for a squid giant axon using a series of mathematical equations. In order to build up the full Hodgkin and Huxley model we first need to characterize the conditions and physiology which makes it possible for a cell to "fire" an action potential. A cell from which an action potential can be elicited is said to be "excitable". In order to describe the properties and behaviour of a cell membrane producing an action potential we will briefly overview some basics of electrical physics and circuit theory. We will then describe how these terms relate to ion channels and the dynamics of the cell membrane. Next we will discuss the techniques Hodgkin, Huxley and others used to measure the electrophysiological properties of neurons. Finally, we will discuss the Equations governing the electrical activity of the cell membrane, developed with the data found using these techniques.

2.2.1   Electrical Physics

Since we will be using a lot of terms from electrical circuit theory to describe the behaviour of ions with respect to the cell membrane, we will begin by defining some relevant terms. First, Q is used to represent a quantity of charge. It is measured in coulombs (C). The charge on Avogadro's number of elementary charges (proton or electron) is called the Faraday constant (F). For example, the amount of charge on one mole of Na^+ is F. The rate of flow of charges is called current (I). It is the derivative of Q with respect to time and is measured in amperes (A). We will use I to represent the rate at which ions flow through protein channels into and out of the membrane.

Potential difference (V or E) is a measure of the work needed to move a small charge between two points. It is measured in volts (V). Potential difference is also referred to as

voltage or simply potential. A change that makes the potential more positive is called a depolarization and a change that makes the potential more negative is called a hyperpolarization. Furthermore, a change that returns the membrane potential to the resting state after the initial depolarization is referred to as a repolarization. Since V and E are both used to represent voltage, in any equations that follow E will be used to represent a voltage that is a constant and V will represent voltage that is a variable. The potential difference we are interested in is the difference in potential across the cell membrane given by the following equation

$$V(t) = V_i(t) - V_e(t) \tag{2.1}$$

where t represents time and the subscript i denotes the intracellular voltage and e denotes the extracellular voltage.

Conductance (g) measures the ease of flow of current between two points and is measured in siemens (S). The reciprocal of conductance is called resistance (R) and is measured in ohms (Ω). There is a very important relationship between theses quantities which we will be using to model the rate of flow of ions across the membrane. It is known as Ohm's law:

$$I = gV \tag{2.2}$$

A potential difference occurs when there is a separation of charge, i.e., an excess of positive charge on one side and negative charge on the other. Capacitance (C) measures how much charge (Q) needs to be transferred from one conductor to another to set up a given potential difference. It is defined as follows

$$C = \frac{Q}{V} \tag{2.3}$$

or, taking the derivative with respect to time we can also write Equation (2.3) as follows

$$C\frac{dV}{dt} = I \tag{2.4}$$

Capacitance is measured in farads (F). Now we will use these terms to describe the conditions which create an action potential.

2.2.2 What makes a cell excitable?

The cell membrane is composed of a phospholipid bilayer. The polar (charged) heads of the phospholipids are hydrophilic and the non-polar tails are hydrophobic. This causes the heads to face the intracellular space and the extracellular space with the tails in between facing each other. The bilayer is a very thin, 30-50 $\mathring{A}$, insulator which prevents most ions

and other solutes from passing through. The separation of ions allows for there to be different concentrations and amounts of charge on either side of the cell membrane which is fundamental to the creation of action potentials and allows the membrane to modelled as a capacitor.

When the cell is undisturbed the membrane potential is said to be at its "resting potential". The resting potential is quite negative for excitable cells, for example the squid giant axon on which Hodgkin and Huxley experimented had a resting potential of approximately negative 60 mV. When an excitable cell is stimulated, either using a electrode or from receiving a signal by other neurons, there is a resulting transient change in membrane potential as seen in Figure 2.2. For a weak stimulus the membrane potential is perturbed from rest an amount proportional to the strength of the stimulus. However, in excitable cells there is a threshold for which enough depolarizing stimulus will produce a disproportional response. The disproportional response is a non-linear spike known as an action potential and is determined by cell properties rather than the strength of the stimulus. The threshold behaviour is generally true for a reasonable range of inputs, however, there is an upper limit on the amount of current that can be injected into a cell without causing permanent damage. Depending on the cell, a stimulus may result in more than one spike if it is strong enough. The timing between spikes and the rate at which they fire is generally accepted as the way information is conveyed throughout nervous systems.

In order for an action potential to occur the cell needs to be able to selectively allow specific ions to pass through it. This is accomplished through ion channels. These are proteins embedded in the membrane which allow specific ions to flow along the electrochemical gradient. The electrochemical gradient is the combination the forces due to the electrical charge and chemical concentrations, positive ions will move towards an area of the opposite charge and ions will also move from an area of high concentration towards an area of lower concentration. There are also ion pumps which actively use energy to move ions into and out of the cell against their electrochemical gradient. Pumps are generally used to maintain the proper distribution of ions across the membrane for eliciting action potentials. The opening and closing of ion channels is responsible for the transient spike in the membrane potential known as an action potential. It is interesting to note that Hodgkin and Huxley were not aware of a specific mechanism that changed the permeability of the membrane due to the limits of microscopes in the late 1940's.

Since the membrane acts as a barrier between the intracellular and extracellular fluid, it allows for there to be different concentrations of ions on either side of the membrane. There are two properties that we consider affecting the movement of ions. The first is the movement of ions due to a concentration gradient. This causes ions in a high concentration area to diffuse to an area of lower concentration. We assume that the concentration gradient does not change significantly as ions flow across the membrane. The second is the electrical force due to the charge of the ions causing like charges to repel and opposite charges to attract. These two forces are in constant conflict and the potential at which they are balanced is known as the Nernst equilibrium. We will see later that the Nernst equilibrium is a special case of the more general equations governing the movement of ions.
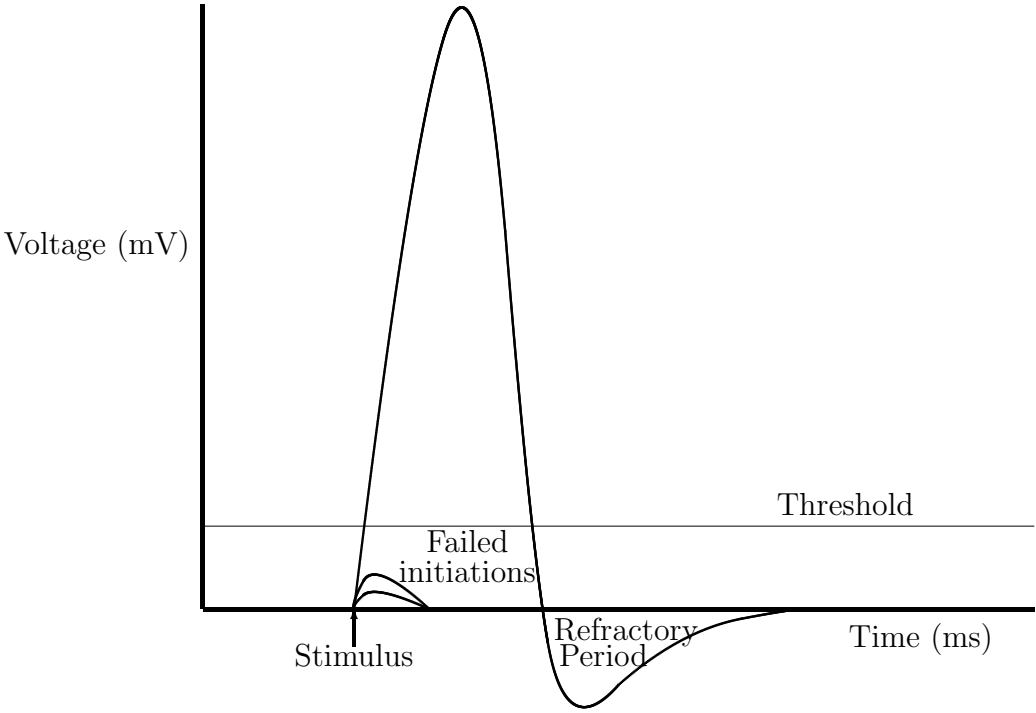
6

Figure 2.2: Action Potential

In order to describe the dynamics of ions flowing across the membrane one can use the Goldman Hodgkin Katz (GHK) current equation. The GHK current equation is derived by solving the Nernst-Planck Equation for electrodiffusion using the following assumptions: the membrane is a homogeneous substance, the electrical field is constant so that the transmembrane potential varies linearly across the membrane, the ions access the membrane instantaneously from the intracellular and extracellular solutions, the permeant ions do not interact, and the movement of ions is affected by both concentration and voltage differences. For a detailed derivation see Hille [9] or Keener and Sneyd [19]. This Equation describes the current across a particular ion channel I_s with respect to the membrane potential (V) and the concentration of ions inside ($[\text{ion}]_i$) and outside ($[\text{ion}]_o$) of the cell:

$$I_S = z_S^2 P_S \frac{F^2}{RT} \left(\frac{[\text{ion}]_i - [\text{ion}]_o e^{-z_S \frac{VF}{RT}}}{1 - e^{-z_S \frac{VF}{RT}}} \right) \tag{2.5}$$

where z is the valence of the ion, P is the permeability of the membrane, F is Faraday's constant, R is the universal gas constant, and T is temperature in Kelvin. By convention a current where cations flow into the cell is considered positive since it causes a rise in the membrane potential, similarly anions flowing outwards is considered positive. By the same reasoning cations flowing out and anions flowing in give negative currents. If we set the left side of Equation (2.5) to zero we can rearrange and solve for the potential at which the current changes sign. This potential is the Nernst potential given in Equation (2.6). The Nernst potential can also be derived from the Boltzmann Equation, see Hille ([9]). The Nernst Equation is given by

$$E_{ion} = \frac{RT}{zF} \ln \frac{[\text{ion}]_o}{[\text{ion}]_i} \tag{2.6}$$

where R is the universal gas constant, T is temperature in Kelvin, z is the valence of an ion and F is Faraday's constant. The Nernst Equation can be expanded to include multiple ions across a membrane and their relative permeabilities across the membrane [9]. However the Nernst Equation only describes the membrane potential at equilibrium for a membrane permeable to a particular ion and does not describe the ion dynamics in detail.

The Nernst Equation does provide a very simple way of thinking about the action potential. Given that the Na$^+$ Nernst potential is +30 mV and the K$^+$ is -60 mV. If the membrane suddenly becomes permeable to only sodium the membrane potential will go to the equilibrium value of +30 mV, then if the membrane potential becomes permeable to only potassium the membrane potential will return to -60 mV. Of course this does not explain the time scale of the dynamics but it provides the basic idea of an action potential being caused by changes in permeability of the membrane.

2.2.3   Measurement Methods

During the 1940's, experiments were done on the giant axon found in a squid that enabled a much greater understanding of how neurons work. We will discuss some of the first methods used to measure the membrane potential and current flowing through the cell membrane of a neuron. These methods were used in the experiments by Hodgkin and Huxley which they used to determine a mathematical model describing the membrane potential, see Section 2.3 . We will also discuss the more modern research methods which generate the data we will use to formulate the bag-cell neuron model.

Current Clamp

Working on the squid giant axon, Marmont [24] was able to achieve isopotentiality over a region of the axon by threading a chloride covered silver wire into the axon to short-circuit the longitudinal resistance in the cytoplasm of the axon. This prevented propagation of the action potential along the axon. The squid giant axon was taken from the stellate nerve of a *Loligo*, which is used to initiate movement when escaping from predators. The squid giant axon was very useful as it is, as the name suggests, gigantic, with a diameter up to 1 mm. Marmont was also able to restrict current measurement to a short segment of the axon by using electrical circuits to set up two "guard" zones on either side of the area he was measuring. These zones ensured that the membrane potential on either side matched the potential of the central region and thus prevented action potentials from outside the central region from propagating in. Marmont used these experiments to inject current into the cell and measure the resulting change in membrane potential. This allowed Marmont to record action potentials in a single patch on the membrane.

Voltage Clamp

The voltage clamp is a simple feedback circuit designed to hold the membrane potential at a specific value, seen in Figure 2.3. This method was developed by Marmont, Cole, and Hodgkin, Huxley, and Katz ([24],[14]). Hodgkin Huxley and Katz improved upon Marmont's method by using different electrodes to measure the internal membrane potential and to inject current.

A voltage clamp experiment works as follows. Two electrodes are inserted into the axon, one records voltage and the other is used to inject current. A third electrode is used to measure the external voltage. The experimenter chooses a voltage at which to hold the cell, and the recorded voltage is compared to this, if the voltages differ then current is injected into the cell to make the membrane voltage equal the holding voltage. The current injected into the cell cancels out the ionic currents in the membrane. Since the voltage is held constant the capacitive current ($I_C = C\frac{dV}{dt}$) is zero. In the case of the squid giant axon a long silver wire was threaded down the length of the axon to maintain the voltage clamp conditions at all locations, this is known as a space clamp.
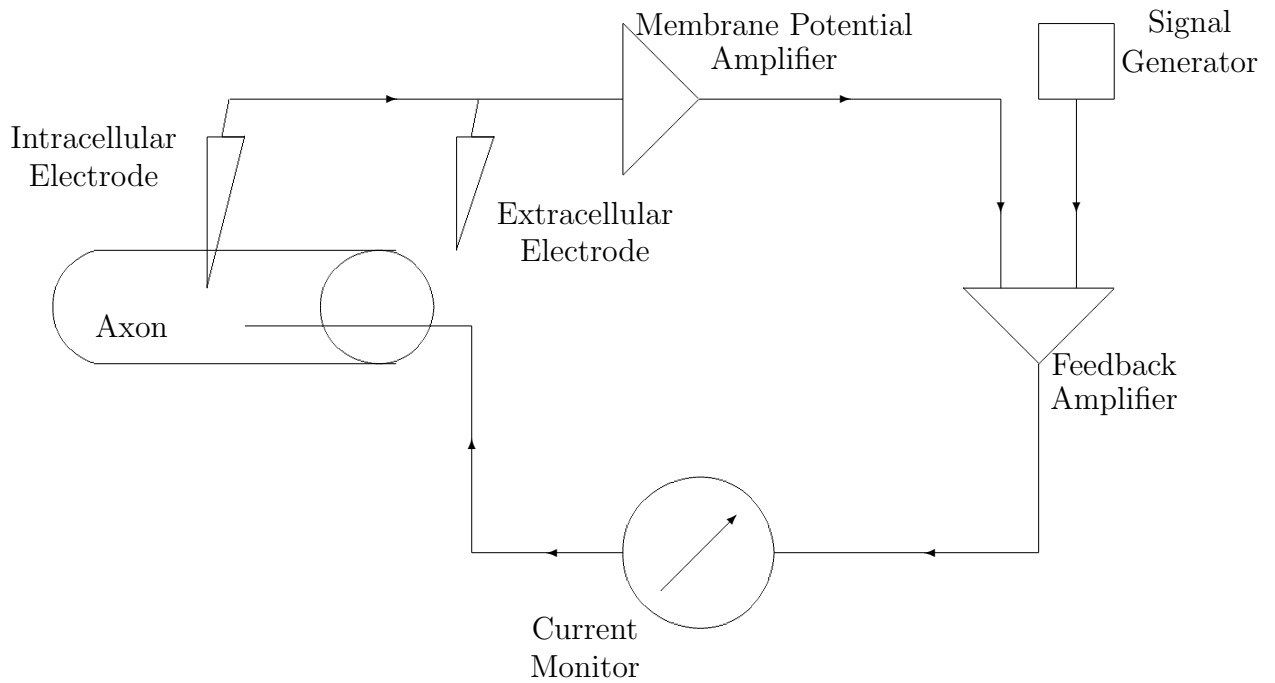
Figure 2.3: Voltage Clamp Apparatus: The membrane potential is measured and fed into an amplifier. The membrane potential is compared with a desired potential and a signal is sent back through into the axon as negative feedback to maintain the desired potential

Modern Research Methods

Modern experiments differ from those discussed above in several ways as the methods for performing voltage clamps and controlling the intracellular solution have improved since Hodgkin and Huxley's seminal work. One method, known as a patch clamp, uses a glass micropipette with an open tip as an electrode which encloses a small portion of the membrane surface area (the "patch"). This technique was developed by Erwin Neher and Bert Sakmann in the late 1970s early 1980's for which they received a Nobel Prize [25]. To make a whole-cell recording a polished glass pipette is placed on the cell and a gentle suction is applied forming a high resistance seal between the pipette and the membrane. Further suction is then applied rupturing the membrane in the area inside the pipette. The interior of the pipette effectively becomes the inside of the cell allowing for an electrode to be inserted to measure the potential and another to input current. A third electrode is used to measure the extracellular potential. Researchers can also use a similar technique to remove a small portion of the membrane as soon as the seal is formed so that they can effectively measure the behaviour of the channel with any "intracellular" and "extracellular" solutions they chose.

In situations where researchers want to measure the potential inside the cell membrane with minimal effect on the ionic constitution of the intracellular fluid a sharp electrode method can be used. These micropipettes are like those for patch clamp, but the pore is much smaller so that there is very little ion exchange between the intracellular fluid and the electrolyte in the pipette.

2.3   Hodgkin and Huxley Model

The following description of Hodkgin and Huxley's work was taken from their original papers, see [14], [11], [10], [12] and [13]. Using the techniques described above, Hodgkin and Huxley were able to hold the membrane potential to a chosen constant value and then change the membrane potential almost instantaneously to a new value and record the resulting change in current. This method is known as the voltage clamp (discussed in detail in Section 2.2.3) and can also be referred to as a step depolarization. Also it is important to note that for a squid giant axon a space-clamp was used which means there was no spatial variation of membrane potential. The voltage clamp offered the first quantitative measure of ionic currents flowing across the membrane. Figure 2.4 shows the type of results that Hodgkin and Huxley saw when they performed a voltage clamp experiment, where at t=0 the membrane potential is changed from its holding value to the clamp value. From the results they determined there must be two currents, an inward current causing the initial drop followed by an outward current causing the rise afterwards.

With this method, Hodgkin and Huxley could separate currents carried by different ions. We know that for membrane potentials less than the Nernst potential a cation will flow inwards (a positive current) and for a membrane potential greater than the Nernst potential a cation will flow outwards (a negative current). Another important experiment using the
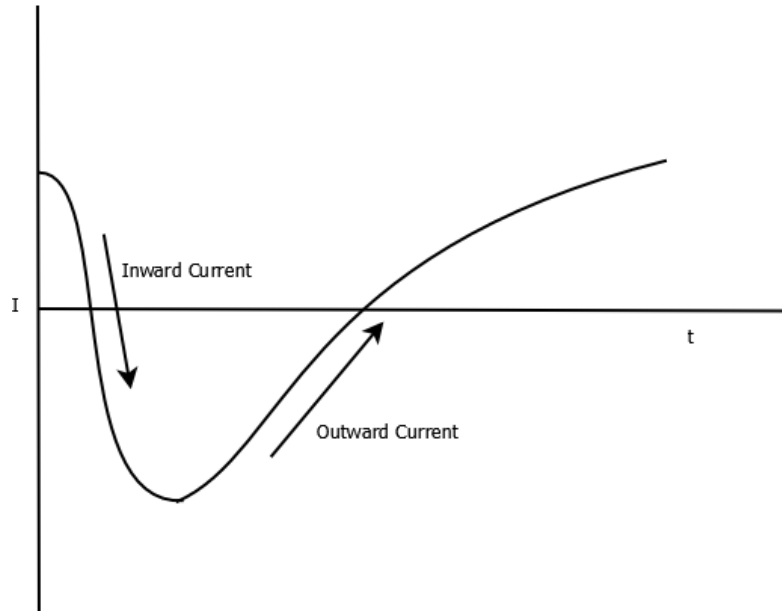
Figure 2.4: Example Voltage Clamp Results for Hodgkin and Huxley

voltage clamp was to remove ions from the extracellular space and replace them with an ion of the same charge that would not permeate the membrane, this allowed Hodgkin and Huxley to determine which ions could permeate the membrane. It was also assumed that an ion's ability to cross the membrane was not dependent on the concentration of other ions. This assumption is valid for the Na^+ and K^+ channels in the squid giant axon, but some more complicated channels can be dependent on the concentration of Ca^{2+} in the cell and other mechanisms as we will see later. Hodgkin and Huxley were able to use these methods to determine which ions were responsible for carrying currents across the membrane. For example the Hodgkin and Huxley paper [11] tested their hypothesis that sodium carried an inward current by varying the amount of sodium and replacing it with choline (a non-permeant ion) in the extracellular solution and comparing the results of the voltage clamp experiments. They found that the early inward current portion of the results (seen in Figure 2.4) disappeared with the lack of sodium. They were able to perform similar experiments with potassium to determine it was responsible for the outward current portion of the results. Hodgkin and Huxley also noticed a small, relatively voltage independent component of the current which they called the leak current.

Once Hodgkin and Huxley had determined the ionic currents, the next step was to give a quantitive measure to relationship between current and membrane potential for each current. They did this by measuring what they called the "instantaneous current-voltage relation":they held the membrane potential at a slightly depolarized value and then stepping the voltage to a more depolarized value and measured the current immediately after the step. One set of experiments was done with high sodium permeability and one with high potassium

permeability. Both experiments gave an approximately linear current-voltage relationship consistent with Ohm's Law. Thus Hodgkin and Huxley introduced ionic conductances as measures of membrane permeability defined in terms of ionic current as follows

$$I_{Na}(V) = g_{Na}(V)(V - E_{Na}) \tag{2.7}$$
$$I_K(V) = g_K(V)(V - E_K) \tag{2.8}$$

Linearity is only an approximation but it is valid for these ions over the voltage range that occurs during normal cell activities. This can be confirmed empirically and from the Goldman Hodgkin Katz current Equation. Conductance, like current is voltage and time dependent. Using the above Equations combined with voltage clamp experiments we can determine the relationship between conductance and voltage.

In order to model the behaviour of the cell membrane it is very useful to describe the membrane potential in terms of an electrical circuit. The circuit consists of three components analogous to the different parts of the physical system. Conductors or resistors are used to represent the ion channels, batteries to represent the concentration gradients of the ions, and capacitors to represent the ability of the membrane to separate charge. The circuit equivalent which reproduces the behaviour of the membrane potential is a capacitor in parallel with resistors and batteries representing each ion channel, as seen in Figure 2.5. We can apply Kirchoff's Current Law, that the sum of the currents flowing into or out of a node must be zero, to conclude that the capacitive current, the ionic currents, and the applied current must sum to zero.

$$I_C + I_{ion} - I_{app} = 0 \tag{2.9}$$

Using Equation (2.4), we can replace I_C to obtain

$$C\frac{dV}{dt} + I_{ion} - I_{app} = 0 \tag{2.10}$$

where C is the membrane capacitance, V is the membrane potential, I_{app} is the applied current, and I_{ion} is the sum of the currents due to the various ion channels. It is important to note that charge cannot actually flow across a capacitor but is redistributed across the membrane. Experimentally Equation (2.10) means that the applied current, I_{app}, equals the ionic currents when the voltage is clamped. We replace I_{ion} with the sodium, potassium and leak currents from Equations (2.8) and (2.7) to obtain

$$C\frac{dV}{dt} = -g_{Na}(V)(V - E_{Na}) - g_K(V)(V - E_K) - g_L(V - E_L) + I_{app} \tag{2.11}$$

where g_{Na} and g_K are voltage and time dependent. We will discuss each of the conductances separately, both the Equations governing them and the experiments used to determine the parameters of said Equations.
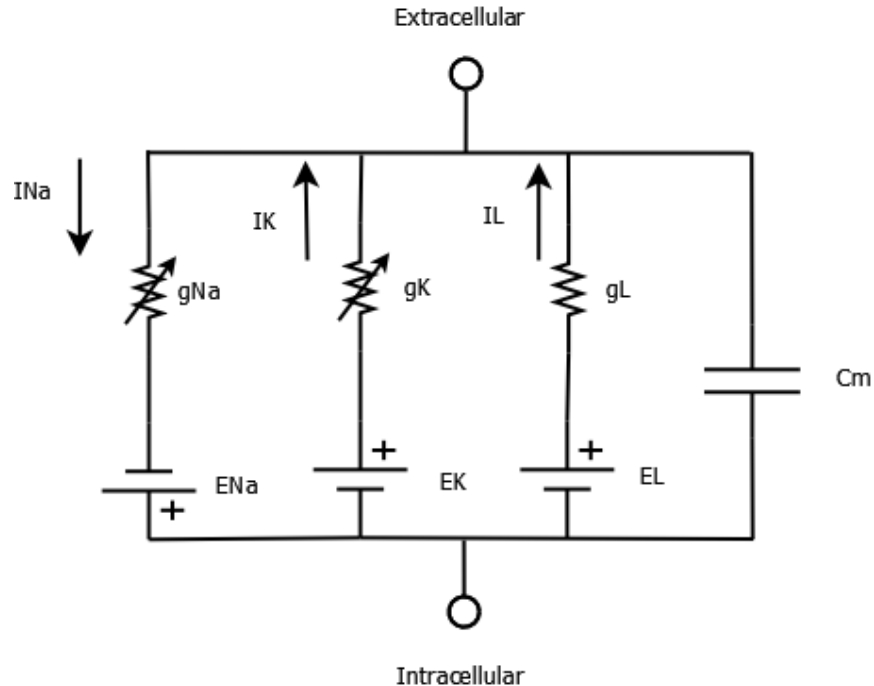
Figure 2.5: Circuit Diagram of Hodgkin and Huxley Model

2.3.1 Leak Current

The easiest current to measure, the leak current can be determined by a voltage clamp experiment that hyperpolarizes the cell. When the membrane potential is far enough below the resting potential all of the voltage gated ion channels are closed and thus any current observed is due to the leak current. Since non-specific channels are mostly permeable to potassium, the reversal potential for the leak tends to be near E_K. In addition the sum of the ion and leak currents are zero at the resting potential so we can determine the values of g_L and E_L since we have two data points and two unknowns.

2.3.2 Potassium Conductance

First we will describe the potassium conductance because it has the simpler behaviour of the two voltage dependent ion channels. Hodgkin and Huxley were able to remove the sodium from the bathing solution and replace it with a non-permeant ion and thus eliminate the inward sodium current during voltage clamp experiments but keep the distribution of charge the same. With the sodium current off and the leak current known we can subtract it away to isolate the potassium current. From Equation (2.8), by dividing the current by $(V - V_K)$ Hodgkin and Huxley obtained data for the potassium conductance at different voltages. Hodgkin and Huxley proposed the following Equation to represent the potassium

conductance

$$g_K(t) = \bar{g}_K n^4(t) \tag{2.12}$$

where the fourth power was chosen in order to best fit the data, $\bar{g}_K$ is the maximal conductance and n is a dimensionless variable that varies between 0 and 1 and represents a fictional activation particle. In current research, n^4 is thought of as the proportion of ion channels open or the probability of a channel being open. It follows that 1-n is the probability of finding a channel closed. Assuming only these two states exist we can write the first order kinetics as follows

$$O \underset{\alpha_n}{\overset{\beta_n}{\rightleftharpoons}} C \tag{2.13}$$

where O represents the proportion of open channels and C represents the proportion of closed channels. α_n is a voltage-dependent rate constant, measured in msec^{-1} that determines how quickly the channel transitions between closed and open states. Similarly β_n is a voltage-dependent rate constant determining how quickly the channel transitions between open and closed states. This corresponds to the following differential Equation

$$\frac{\mathrm{d}n}{\mathrm{d}t} = \alpha_n(V)(1-n) - \beta_n(V)n \tag{2.14}$$

These Equations can be derived stochastically [20]. Instead of using α_n and β_n, we can express Equation (2.14) in terms of the voltage-dependent steady state value $n_\infty(V)$,and the voltage-dependent time constant $\tau_n(V)$ as follows

$$\frac{\mathrm{d}n}{\mathrm{d}t} = \frac{n_\infty(V) - n}{\tau_n(V)} \tag{2.15}$$

where

$$n_\infty(V) = \frac{\alpha_n(V)}{\alpha_n(V) + \beta_n(V)} \tag{2.16}$$

and

$$\tau_n(V) = \frac{1}{\alpha_n(V) + \beta_n(V)} \tag{2.17}$$

At the resting state ($V = 0$ mV in Hodgkin and Huxley's original papers) n has a resting value of

$$n_\infty(0) = \frac{\alpha_n(0)}{\alpha_n(0) + \beta_n(0)} \tag{2.18}$$

We can now solve Equation (2.15) with the initial condition (2.18)to find $n(t)$ when the voltage is clamped to a new value, V_{Clamp}

$$n = n_\infty(V_{clamp}) - (n_\infty(V_{clamp}) - n_\infty(0)) \exp^{-\frac{t}{\tau_n(V_{Clamp})}} \tag{2.19}$$

This equation can be rewritten in terms of conductance by multiplying by $\bar{g}_K$ to better compare to the experimental results

$$g_K = \{g_{K\infty}^{\frac{1}{4}} - (g_{K\infty}^{\frac{1}{4}} - g_{K0}^{\frac{1}{4}}) \exp^{-\frac{t}{\tau_n}}\}^4 \tag{2.20}$$

The data was fit for a large range of voltage clamp experiments . The maximal value for the conductance was taken to be 20% greater than the steady state result of the -100mV clamp where it was assumed n would be 1. Hodgkin and Huxley then fit expressions for $\alpha_n(V)$ and $\beta_n(V)$ to the data. The final Equation for the potassium current is

$$I_K = \bar{g}_K n^4(t)(V - E_K) \tag{2.21}$$

with $n(t)$ determined by Equation (2.14)

2.3.3 Sodium Conductance

The sodium conductance rises rapidly and then decays during a step depolarization. This is due to the sodium channel having both a voltage gated activation component as well as an inactivation component. If there were no inactivation component the conductance would simply rise to a new steady state value at the depolarized voltage. Once inactivation has occurred the membrane potential has to be repolarized or hyperpolarized to remove the inactivation effects. In order to model the two components, Hodgkin and Huxley chose to have two variables, one representing activation and the other inactivation. They assumed Equations of the form

$$g_{Na}(t) = \bar{g}_{Na} m(t)^3 h(t) \tag{2.22}$$

$$\frac{\mathrm{d}m}{\mathrm{d}t} = \alpha_m(V)(1 - m) - \beta_m(V)m \tag{2.23}$$

$$\frac{\mathrm{d}h}{\mathrm{d}t} = \alpha_h(V)(1 - h) - \beta_h(V)h \tag{2.24}$$

Similar to the potassium conductance case, m^3h represents the proportion of channels open. Where m governs the activation component and h governs the inactivation component. Hodgkin and Huxley noted this could be done with a single variable with a second order Equation but they felt it was more straightforward to model the dynamics using two first order variables. Similar to the potassium conductance we can solve Equations (2.23) and (2.24) with initial condition at the resting potential to get

$$m = m_\infty - (m_\infty - m_0) \exp^{-\frac{t}{\tau_m}} \tag{2.25}$$

$$h = h_\infty - (h_\infty - h_0) \exp^{-\frac{t}{\tau_h}} \tag{2.26}$$

Hodgkin and Huxley noted that at rest the sodium conductance values were very small compared to during large depolarizations so m_0 could be neglected. Also they found that inactivation does not occur for low voltages, i.e. $h_\infty \approx 1$. Combining these two results gave the following Equation for conductance

$$g_{Na} = \bar{g}_{Na} m_\infty^3 h_0 [1 - \exp^{-\frac{t}{\tau_m}}]^3 \exp^{-\frac{t}{\tau_h}} \qquad (2.27)$$

From the data, Hodgkin and Huxley obtained values for $\bar{g}_{Na}, m_\infty, h_0, \tau_m,$ and τ_h. Hodgkin and Huxley measured h_∞ using a two-pulse voltage clamp experiment. The cell is held at a prepulse potential long enough for the inactivation to reach a steady state. Then the cell is stepped up to a higher potential and compared to results from the activation voltage clamp to determine the percentage of channels that are closed.

2.3.4 Full Model

Combining the results for these currents, Hodgkin and Huxley were able to describe the action potential of a squid giant axon . The model is still a widely accepted model of action potential generation, and the methods and model can be used to describe may different neurons and their action potentials. The work won them the 1963 Nobel Prize in Physiology and Medicine. In Chapter 4 we use their work as the basis for creating a model describing the membrane potential of a bag-cell neuron in an Aplysia.

Chapter 3

Background on Aplysia

3.1 Aplysia Biology

An Aplyisia is a genus of marine mollusk commonly called a sea slug or sea hare. It is known as a sea hare due to its round shape and two club shaped structures protruding upwards from their head that resemble the ears of a hare. The Apylsia Californica has been known to grow as large as 75 cm when fully extended. Other Aplysia, such as Aplysia vaccaria, have been known to grow even larger. As the name suggests Aplysia Californica can be found in the sea off the coast of California as well as northern Mexico and Florida. Aplysia California are herbivores with a diet consisting mostly of red algae. When disturbed, sea hares are capable of releasing a reddish-purple ink as a defence mechanism.

Aplysia are hermaphroditic and play the role of both male and female during mating. During egg laying the Aplysia finds a vertical surface to climb and begin a series of predictable behaviours that culminate in egg laying. A single egg mass may contain over 100 million eggs. Aplysia are very prolific egg layers and a single Aplysia has been reported to lay over as many as 478 million eggs during a period of just over four months. Egg laying is a seasonal activity and it is known to be dependent on the temperature of the sea water. The natural stimulation for egg laying is unknown although it has been suggested that egg laying Aplysia release a pheromone that causes other Aplysia to begin laying eggs.

Aplysia are of much interest in neurobiology due to the simplicity of their central nervous system which consists of approximately twenty thousand neurons, a relatively small number compared to the human brain. The egg laying behaviour of an Aplysia is very interesting to neuroscientists due to the role of bag-cell neurons, which when firing repetitively release a hormone that causes the onset of a series of behaviours culminating in egg laying. Aplysia have also been very useful in the study of learning and memory, specifically the work of Nobel laureate Eric Kandel on how neurons are able to form and store memories.
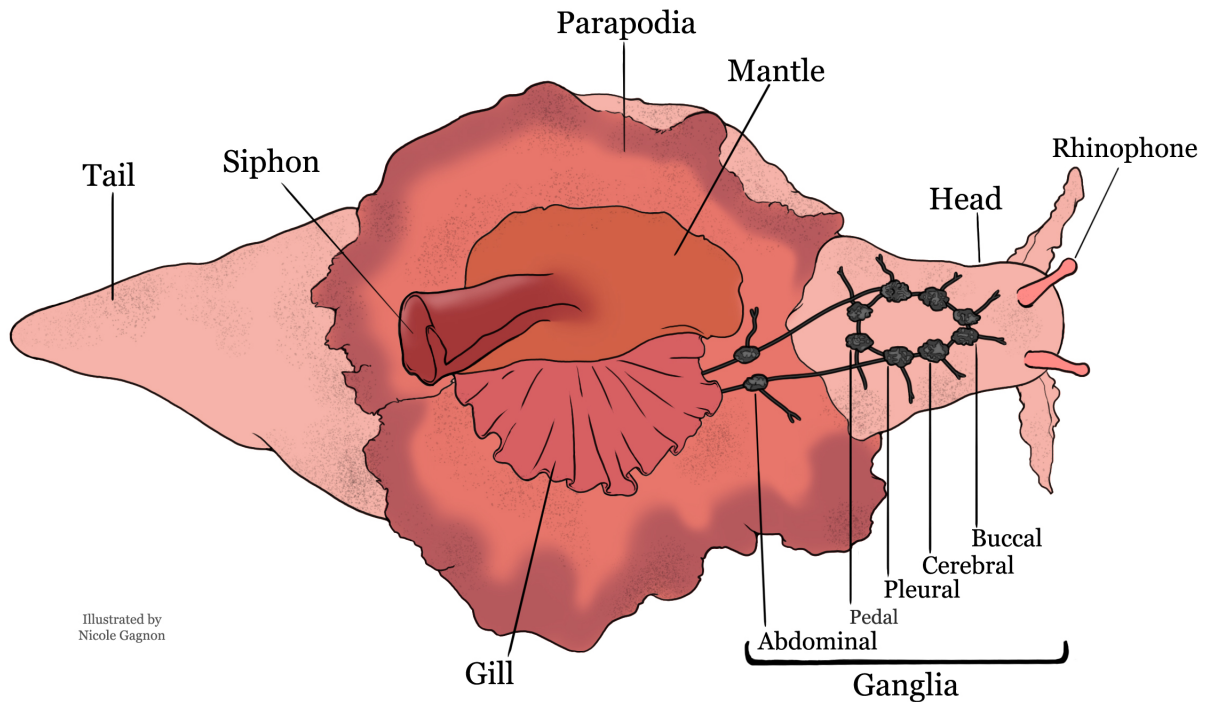
Figure 3.1: Aplysia diagram showing the location of the abdominal ganglion

3.2 Bag-cell Neuron

The following description of bag-cell follows the information from Kaczmarek and Conn [2]. Bag-cell neurons are important to study due to their direct link between the behaviour of the neuron and the behaviour of the animal. Due to the simplicity of the animal's nervous system it is easier to understand the role of the neurons in relation to the behaviour of the animal. Furthermore bag-cell neurons are well suited for traditional techniques for studying neurons using biochemistry, electrophysiology and molecular biology. Bag-cell neurons are located in the abdominal ganglion of an Aplysia. A ganglion is a term for a group of nerve cells. The various parts of the Aplysia central nervous system are labeled in Figure 3.1. Bag-cell neurons form two bilaterally situated clusters of 200 to 400 cells at the rostral end of the abdominal ganglion. Bag-cell neurons are named due to their shape. Bag-cell neurons are multipolar and send their processes (dendrites or axons) in all directions into the surrounding connective sheath. Each neuron has two or three processes that extend from the soma and branch extensively. The majority of processes group together and extend into the pleuroabominal connective nerve and wrap around the proximal portion to form a "cuff". A small number of neurons extend up the pleuroabdominal connective among the axons of other cells. Also, most bag-cell neurons extend one or more branches over the abdominal ganglion or towards the contralateral bag-cell cluster. Bag-cell neurons contain

19

round peptidergic granules throughout the cell, and especially dense clusters can be found near the axon terminal. These vesicles mostly contain the neuropeptide egg laying hormone (ELH). Bag-cell neurons release ELH both locally to other neurons and into circulation. The previously mentioned extension of the bag-cell processes into connective tissue could allow for the vesicle contents to be released into general circulation.

Bag-cell neurons have three states: a resting state where action potentials can be elicited, the afterdischarge state where the cell fires spontaneously, and a refractory state where the cell cannot be stimulated into the after discharge state. The resting potential of the bag-cell neuron is between -40 and -65 mV. Action potentials can be elicited with an intracellular depolarizing current stimulating the cell. The action potential of the resting cell does not have the same all-or-nothing type response seen in other neurons. In the case of a bag-cell neuron the upstroke of the spike only persists as long as their is a depolarizing stimulus current. As soon as there is no stimulus current, and in some cases before the stimulus current is turned off, the membrane potential starts to return to the resting value. Long depolarizing pulses can cause the cell the "spike" more than once. The spikes have a duration ranging from 30 to 150 ms.

A stimulus to the pleuroabdominal nerves or a repetitive stimulus to the bag-cell neurons themselves can cause a change in the electrical properties of the cell allowing for it to fire constantly for up to 60 minutes, although more often it only fires for 30 minutes. The behaviour where the cell fires constantly is called the afterdischarge. The afterdischarge is thought to be a tightly regulated all-or-nothing event in which the amount of stimulus does not effect the duration of the afterdischarge. During the afterdischarge the neurons release the neurotransmitter ELH which does not occur during spikes otherwise. Bag-cell neurons are electrically coupled which causes the clusters to fire in tight synchrony during the afterdischarge event. The evidence for the coupling between neurons comes from the injection of lucifer yellow dye into a single neuron and then observing that the dye labels adjacent cells. The coupling is thought to be in the form of a gap junction. Not only are the neurons within a cluster electrically coupled, but the two clusters are also coupled. The coupling means that one cluster can act as a pacemaker for the other. The synchrony in firing during the afterdischarge could be to ensure that all cells within a cluster are firing and thus there is a maximal output of neurotransmitter. The afterdischarge event begins with high frequency firing of action potentials (2-6 Hz) for less than one minute followed by a relatively low frequency of less than 0.5/min that lasts for the rest of the afterdischarge. During the afterdischarge the shape of the action potentials changes, become taller and wider early during the second phase. In vivo the mean duration of the discharges has been found to be 21 minutes. Following the afterdischarge bag-cell neurons enter a prolonged inhibitory state. The inhibitory state occurs gradually but it takes up to 20 hours before another full-length afterdischarge can be elicited. It has been observed that there is a delay of roughly 30 minutes between the end of the afterdischarge and the onset of egg laying behaviour.

The afterdischarge event is thought to be influenced by several secondary messenger molecules which help cause the long-lasting changes in the electrical properties of the cell. Cyclic AMP plays a key role in the generation of bag-cell afterdischarge. After the onset

of the event, the levels of cAMP rise and the excitability of cell has been shown to change. Specifically cAMP seems to decrease the net outward currents. Protein Kinase C (PKC) has also been shown to increase during the afterdischarge and PKC has been shown to enhance the inward calcium current (responsible for helping depolarize the cell during a spike). The enhanced calcium current seems to be due to a covert calcium channel that only becomes active during the afterdischarge. These secondary messengers will be discussed in more detail in the next section.

3.3   Aplysia Bag Cell Neuron Literature

We will start by looking at the experiments done on bag-cells over the last 30 years. In order to build a complete model of the bag-cell neuron we need to look at the different ion channels present in bag-cells. We will discuss the results of the literature chronologically starting with some of the first analyses of the bag-cell action potentials and afterdischarge behaviour followed by individual current analyses.

3.3.1   Kupfermann and Kandel 1970, Kupfermann 1970

In two papers in 1970, Kupfermann investigated the properties of the bag-cell neuron. The first paper with Kandel [22] investigated the electrophysiological properties of the neurons. These experiments were done by isolating the abdominal ganglion of the Aplysia and pinning it in a dish of artificial seawater solution. The authors then used glass micropipettes to impale the cells, inject current and record the response from the cells. They discovered the cells were mostly silent with some cells spontaneously firing. Depolarizing pulses were used to elicit action potentials with a spike height of roughly 80 mV lasting for 30-150 ms. However a train of pulses could be used to stimulate most cells into repetitive firing which lasted for more than 5 minutes with a maximum duration of 55 minutes. It was discovered that a large fraction of the spikes occur within the first few minutes of the afterdischarge and it was observed that there was no obvious correlation between the number of spikes in the afterdischarge and the preceding stimulus. After the afterdischarge the cells became silent and a new burst of activity could not be started for up to an hour. The authors confirmed that the cells could not be stimulated antidromically (action potential travelling in the opposite direction, from axon towards the soma) to determine that afferent fibers in the connective close to the pleural ganglion were not responsible for the afterdischarge stimulation. The cells were found to always fire synchronously but did not require the other cell cluster to exhibit the afterdischarge effect, however the afterdischarge was shorter in length when the two bag-cell clusters were disconnected. The authors also eliminated the possibility of a driver interneuron by showing the same behaviour occurred in a bag-cell isolated from its cluster. The second paper by Kupfermann ([21]) investigates and confirms the release of a hormone from bag-cells that stimulates egg laying. Kupfermann homogenized bag-cells

from an Aplysia and injected the bag-cell extract into live Aplysia and found that egg laying behaviour occurred within 2 hours for 66.7% of the animals.

3.3.2   Strong 1984: A-current

In a 1984 paper ([31]), Strong studied the transient outward potassium current, also known as the A-current, under the effects of specific drugs. The A-current has properties similar to the sodium current in the Hodgkin and Huxley model in that it activates when the membrane potential is depolarized and then inactivates shortly afterwards. The predominant role of the A-current is to determine the behaviour of the cell at lower voltages. The excitability of the bag-cell neuron is thought to be affected by internal levels of intracellular adenosine 3':5' -monophosphate (cAMP) (Kaczmarek 1978 [16]). Strong investigated the effect of increasing the internal cAMP level on the A-current by applying forskolin (an activator of adenylate cyclase) and RO20-1724 (a phophodiesterase inhibitor or PDI) and taking voltage clamp measurements of the cell. Specifically forskolin and the PDI mimic the effects of cAMP and have been found to initiate afterdischarges in intact bag-cell clusters (Strumwasser et al. 1982 [33]). Forskolin and the PDI have also been found to enhance the width and height of action potentials (Kaczmarek and Kauer 1983 [17]) and raise the internal levels of cAMP. Since the A-current occurs at much lower potentials than other currents it can be isolated from other potassium currents by limiting the study to more negative potentials.

The application of forskolin and the PDI were reported to substantially speed up the inactivation kinetics but they do not affect the steady state behaviour of the activation or inactivation. The other major effect was the lowering of the peak potential at all voltages in the clamp experiment. The effects of forskolin could be at least partially reversed by washing out the bathing solution of the neuron.

3.3.3   Strong 1986: K1 and K2 Current

In a 1986 paper ([32]) Strong performed similar experiments to those in Strong 1984 ([31]) on the other outward currents in a bag-cell. These currents are thought to be responsible for the repolarization behaviour of the cell during an action potential. Strong used ethylene glycol tetraacetic acid (EGTA) to block the intake of calcium into the cell and prevent the presence of a calcium activated potassium current. Voltage clamp experiments similar to [31] were carried out both with and without forskolin and a PDI. Strong noticed that the tail current in the results could not be described with a single decaying exponential. However, the tail current could be described by the sum of two exponentials, which suggests that there are two channels or a single channel with complex kinetics. The hypothesis of two channels was supported by the fact that the two inactivation rates were affected differently by the presence of forskolin. The two currents are carried by potassium ions and are labelled I_{K1} and I_{K2}. I_{K1} is an non-inactivating outward potassium current, whereas I_{K2} has an inactivation component. I_{K2} was determined to be a different current to I_A due to it being

active at different range of membrane potentials and having different kinetics.The effects of forskolin and the PDI were similar to the A-current, I_{K1} and I_{K2} had a decreased peak current value during voltage clamp experiments and substantially faster inactivation.

3.3.4   Conn, Strong, Kaczmarek 1989: PKC

In a 1989 paper ([3]), Conn, Strong and Kaczmarek investigated the secondary messenger Protein Kinase C and determined it was responsible for recruiting a previously covert species of voltage-dependent calcium channel, resulting in an increase of calcium current during the afterdischarge. The PKC current was investigated by introducing PKC activators such as TPA and recording the results. Voltage clamp experiments were performed where the addition of TPA increased the amplitude of the results and then Sphinganine, which inactivates TPA, was used return the cell to normal. Sphinganine was also shown to prevent the enhancement of action potentials when introduced before TPA.

3.3.5   Quattrocki 1994: Cloned K2 Current

A more thorough investigation of the I_{K2} current was done by Quattrocki et al. in 1994 ([27]). Quattrocki's paper provides a separation of I_{K1} and I_{K2} into two distinct currents. The paper investigates the cloning of a channel in the Aplysia which they call Shab and then shows that the cloned current is in fact the same current as I_{K2}. To measure the Shab current the DNA was isolated and then expressed in Xenopus oocytes. I_{K1} and I_{K2} occur in greatly varying ratios in bag-cells and the authors used cells that were expressing primarily one current or the other in order to get separate voltage clamp data. The Shab and I_{K2} currents are compared and determined to be the same as they give similar results in voltage clamp experiments. The reaction of the two similar currents to tetraethylammonium (TEA), which blocks certain types of potassium current inactivations, was also the same. The I_{K2} and Shab currents also display progressive inactivation with repeated depolarization as seen in the previous Strong paper. The authors also created a basic Hodgkin Huxley type model of the bag-cell action potential which will be discussed in detail in Section 3.4.1

3.3.6   Zhang 2002 and 2004: Calcium Dependent Potassium Current

In 2002 and 2004 Zhang et al. ([37],[36]) released two papers which investigated the properties of a calcium dependent outward potassium current, I_{KCa}. I_{KCa} is a type of current that can be blocked by the drug paxilline, which does not block I_A, I_{K1} and I_{K2}. The ability to manipulate the internal and external calcium concentrations allowed for the authors to confirm that there is a calcium dependent current. Furthermore they subtracted the paxilline voltage clamp experiment from the control voltage clamp experiment to obtain a difference

current which consisted of only I_{KCa}. The rest of the paper examines the behaviour of I_{KCa} during the afterdischarge and the effects of the secondary messenger protein kinase C (PKC) on I_{KCa}.

The 2004 Zhang paper looked at two forms I_{KCa} that are the expressions of slo-a and slo-b genes. The slo-a type is determined to be present in adult Apysia and is affected by the secondary messenger protein kinase A (PKA). The slo-b variant is not affected by PKA. Since the genes were used to express a single kind of channel in an oocyte the authors were able to perform voltage clamp experiments on just I_{KCa} and measure the increase in current due to internal calcium levels. Juveniles do not have the slo-a version of IKCa and are unable to initiate an afterdischarge leading the authors to propose that the slo-a version of I_{KCa} is fundamental to the repetitive firing behaviour seen during an afterdischarge.

3.3.7 Hung and Magoski 2007: Calcium Current and Prolonged Depolarizing Current

Magoski 2007 ([15])investigates the presence of a prolonged depolarizing current (I_{PD}) that is responsible for raising the membrane potential to help cause repetitive firing. The membrane depolarization occurs after the cell has been repeatedly stimulated (i.e. a 5 hertz input for 10 seconds). The depolarizing current is thought to be dependent on a secondary messenger calmodulin. Calmodulin is activated by intracellular calcium concentration. In order to measure the effects of Ca^{2+} on the depolarizing current the authors did whole cell voltage clamp experiments where the K^+ and Na^+ ions were replaced with non-permeable ions. The authors confirmed there is a window or limit of Ca^{2+} which causes the depolarizing current to come on. The depolarizing current was determined to be a nonspecific cation current.

3.4 Modelling Literature

3.4.1 Quattrocki et al. Bag Cell Neuron Model

Quattrocki et al. [27] created a model containing a generic calcium current, a leak current, and the Shab potassium current using equations similar to the Hodgkin and Huxley model (see Section 2.3. The governing equation of the Quattrocki model is:

$$C\frac{dV}{dt} = -\bar{g}_{Ca}n^3 j(V - 50) - \bar{g}_K m^4 h(V - (-80)) - \bar{g}_L(V - E_{rest}) + I_{stim} \qquad (3.1)$$

where $C = 0.5nF$, $\bar{g}_{Ca} = 1.2\mu S$, $\bar{g}_K = 0.15\mu S$, $\bar{g}Ca = 0.025\mu S$. Simulations were run with E_{rest} at $-80mV, -60mV$, and $-40mV$ to determine if action potentials would still fire at different membrane resting potentials. I_{stim} represents the stimulus current injected into the cell and varied from $0 - 0.2$ nA. The differential equations for n ,j , and m are similar to the ones used by Hodgkin and Huxley, see equation (2.15). The maximal conductances, $\bar{g}_i$,

can be thought of to represent the relative strengths of the currents and it is interesting to note that $\bar{g}_{Ca}$ is 8 times the size of $\bar{g}_K$. The variable h differs from the Hodgkin and Huxley equations in that a second order differential equation was used to represent the inactivation of the potassium current. This is due to a very steep inactivation at first followed by a slower inactivation that cannot be fit well by a single exponential function. This is represented by the following kinetic equation

$$p \underset{\alpha_1}{\overset{\beta_1}{\rightleftharpoons}} q \underset{\alpha_2}{\overset{\beta_2}{\rightleftharpoons}} h \tag{3.2}$$

where p is the permissive state and both q and h are inactive states. The kinetics correspond to the following differential equations

$$\frac{dq}{dt} = \alpha_1 - (\alpha_1\beta_1 + \alpha_2)q + (\alpha_2\beta_2 - \alpha_1)h \tag{3.3}$$

$$\frac{dh}{dt} = \alpha_2 q - \alpha_2\beta_2 h \tag{3.4}$$

The results were a model that recreated the single spike behaviour of the bag-cell neuron very well. The calcium current from another cell and lack of I_{K1} and other potassium currents mean the model does not fully represent bag-cell behaviour physiologically. It is only meant to represent the shape of a single spike. The spike itself does not have the typical behaviour of an action potential as it is not an all or nothing event. The membrane potential only depolarizes while the the stimulus current is on and will drop as soon as the stimulus is turned off. In Figure 3.2 we simulated the model using the equations and parameters given in [27]. We found that we needed to increase the stimulus current from the value of 0.2 nA they used and were able to obtain a similar spike.

3.4.2   Canavier et al. R15 Neuron Model

Since there are no previous full models for the Aplysia bag-cell neuron, we will look at a neuron from the same animal, the R15 neuron. The R15 neuron is located in the abdominal ganglion and has been useful in gaining insight into the biophysical mechanisms underlying bursting behaviour in neurons. Bursting behaviour is when a cell fires repetitively for a finite amount of time followed by a quiescent period and then the behaviour repeats itself. With enough stimulation the cell has been known to fire continuously. This is known as beating. Most of the R15 model is similar to a typical Hodgkin Huxley type model.

The governing equation for the membrane voltage is

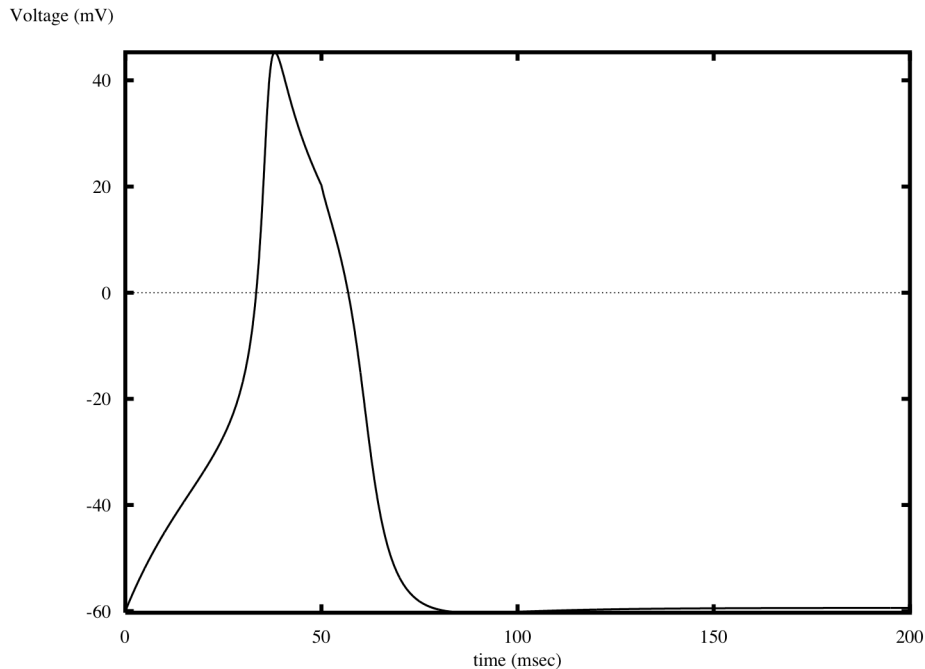$$C\frac{dV}{dt} = -\sum I_i + I_{app} \tag{3.5}$$

Figure 3.2: Quattrocki Model Spike

where the index i represents several currents which we will not describe in much detail here, for more detail see Canavier et al 1991 [1]. There is an inward sodium current I_{Na} and as in the Hodgkin and Huxley model it contributes to the upstroke of the action potential. Unlike the Hodgkin and Huxley model there is also an inward calcium current that is modelled in a similar way with both voltage dependent activation and inactivation. There is a nonspecific cation current to help simulate the depolarizing aftercurrent seen in bursting neurons. There is also a leak current as seen in the Hodgkin and Huxley model that is mainly an amalgamation of other currents that are not very strong in the R15 neuron and helps determine the resting potential. There are also potassium currents, I_K, that is responsible for repolarization during an action potential and I_R which is similar to the previously mentioned A-current.

The main difference from the Hodgkin Huxley model is a slow inward current. The slow inward current is a voltage activated and Ca^{2+} inactivated. In the paper the current is assumed to be carried by calcium ions. The model also represents the internal calcium dynamics by combining the effects of a calcium current, the slow inward current, a sodium-calcium exchanger, a calcium pump and an internal calcium buffer. This results in the following equations

26

$$[\dot{Ca}]_i = \frac{\sum w_j I_j}{Vol_i F} - n[B]_i O_c \tag{3.6}$$

where square brackets denote concentration, I_j are the calcium currents and pumps and w_j converts current to calcium ions per seconds, Vol_i is the effective cell volume and F is Faradays constant. The first term governs the movement of calcium due to current. In the second term n is the number of binding sites, B is the buffer, and O_c is the fraction of sites already occupied in the calcium buffer and thus unavailable for use. The second term governs the amount of calcium absorbed into the buffer. The buffer is based on the properties of the calcium binding protein calmodulin and taken from a model for calmodulin in muscle cells since the precise buffering method in R15 neuron was unknown. O_c is governed by a first order kinetics differential equation as follows

$$\dot{O}_c = k_u[Ca]_i(1 - O_c) - k_r O_c \tag{3.7}$$

where the constants k_u and k_r represent the rates of binding and unbinding, respectively.

The model exhibits all the firing behaviours of the R15 neuron and the authors could easily see the connection between calcium (and slow inward current) oscillations and the bursting behaviour. Basically, slow oscillations in intracellular calcium concentrations cause the slow inward current to depolarize the membrane potential in a periodic way causing the membrane potential to cross the threshold and begin firing. If enough stimulus is input the calcium level stays constant but very high and we see beating behaviour where the membrane potential is above the threshold for the entire duration of the test and thus fires constantly. The authors then reduced the model to two variables to analyse the dynamics of the system using phase planes.

Chapter 4

Model

4.1 Introduction

We will start by briefly outlining the full set of equations used in the model to provide a point of reference when we outline the general method which we used to determine the parameters for the model. We will discuss how we used the general method with each ion channel using data taken from previous research as well as discuss the differences between the methods used on specific channels and the general method. Combining these currents we will create a single cell model. We compare the full model to spikes created from actual cells and adjust our model to reflect the experimental results. Due to the fact that all of our data for different currents come from different experiments using different cells measured with varying techniques it is to be expected that parameters will need to be adjusted. This is especially true for the maximum conductance values which determine the relative strengths of the currents which vary from cell to cell due to the difference in the number of channels expressed in a particular cell.

4.2 Model Equations

The equations of the bag-cell neuron model are as follows

$$C\frac{dV}{dt} = -(I_{Ca} + I_{K1} + I_{K2} + I_{KC} + I_A - I_{app}) \tag{4.1}$$

$$I_{Ca} = \bar{g}_{Ca}m_{Ca}^{p_{Ca}}(V)h_{Ca}(V)(V - E_{Ca})$$

$$I_{K1} = \bar{g}_{K1}m_{K1}^{p_{K1}}(V)(V - E_K)$$

$$I_{K2} = \bar{g}_{K2}m_{K2}^{p_{K2}}(V)h_{K2}(V)(V - E_K)$$

$$I_{KC} = \bar{g}_{KC}m_{KC}^{p_{KC}}(V,Ca)(V - E_K)$$

$$I_A = \bar{g}_A m_A^{p_A}(V)h_{Ca}(V)(V - E_K)$$

$$I_L = \bar{g}_L(V - E_L)$$

$$\frac{dm_i}{dt} = \frac{m_\infty(V) - m_i}{\tau_m(V)} \tag{4.2}$$

$$\frac{dh_i}{dt} = \frac{h_\infty(V) - m_i}{\tau_h(V)} \tag{4.3}$$

$$\frac{dm_{KC}}{dt} = \frac{m_\infty(V,Ca) - m_{KC}}{\tau_m(V)} \tag{4.4}$$

$$m_{\infty,i}(V) = \frac{1}{(1 + e^{\frac{V - V_m}{K_m}})} \tag{4.5}$$

$$h_{\infty,i}(V) = \frac{1}{(1 + e^{\frac{V - V_h}{K_h}})} \tag{4.6}$$

$$m_{\infty,KC}(V) = \frac{1}{(1 + e^{\frac{V - V_m(Ca)}{K_m}})}$$

$$\tau_{m,i}(V) = \tau_{m0}\frac{e^{\frac{\delta_m(V - V_m)}{K_m}}}{1 + e^{\frac{(V - V_m)}{K_m}}} \tag{4.7}$$

$$\tau_{h,i}(V) = \tau_{h0}\frac{e^{\frac{\delta_h(V - V_h)}{K_h}}}{1 + e^{\frac{(V - V_h)}{K_h}}} \tag{4.8}$$

where Equation (4.1) is the governing equation similar to the equation used in Hodgkin and Huxley's model, see Equation (2.11). The model has one inward current, I_{Ca}, which is due to a calcium permeable ion channel and is responsible for the upstroke in the action potential. There are four inward potassium channels: I_{K1} and I_{K2} play a role in action potential broadening and repolarization, I_A is responsible for membrane potential behaviour at hyperpolarized values, and I_{KC} is a calcium dependent channel thought to play a role in the overall excitability of the cell. Each current equation has a maximal conductance $\bar{g}_i$ and reversal potential E_i which depends on which ions the channel is permeable to. All of the currents except for the leak current have an activation variable m which range between 0 and 1 and are dependent on the membrane potential, V. For the current I_{KC} the activation variable is also dependent on the amount of calcium inside the cell. The currents I_{Ca}, I_{K2}, and I_A also have voltage dependent inactivation represented by the variable h which ranges between 1 and 0. The dynamics of the activation and inactivation variables are determined by the differential equations (4.2,4.3,4.4). The forms of the steady state activation/inactivation variable, Equation (4.5), and the time constant, Equation (4.8), were taken from Willms 1999 paper [34] . The $m_\infty(V)/h_\infty(V)$ are sigmoidal functions where the parameter $V_{m/h}$

corresponds to the membrane potential at which the function is at $(\frac{1}{2})^p$ its maximum value and the $K_{m/h}$ parameter affects the slope of the function, see Figure 4.2 for example functions. The time constant functions, $\tau_{m/h}(V)$, are bell shaped functions where the value of δ is between 0 and 1 and determines the skewness of the function.
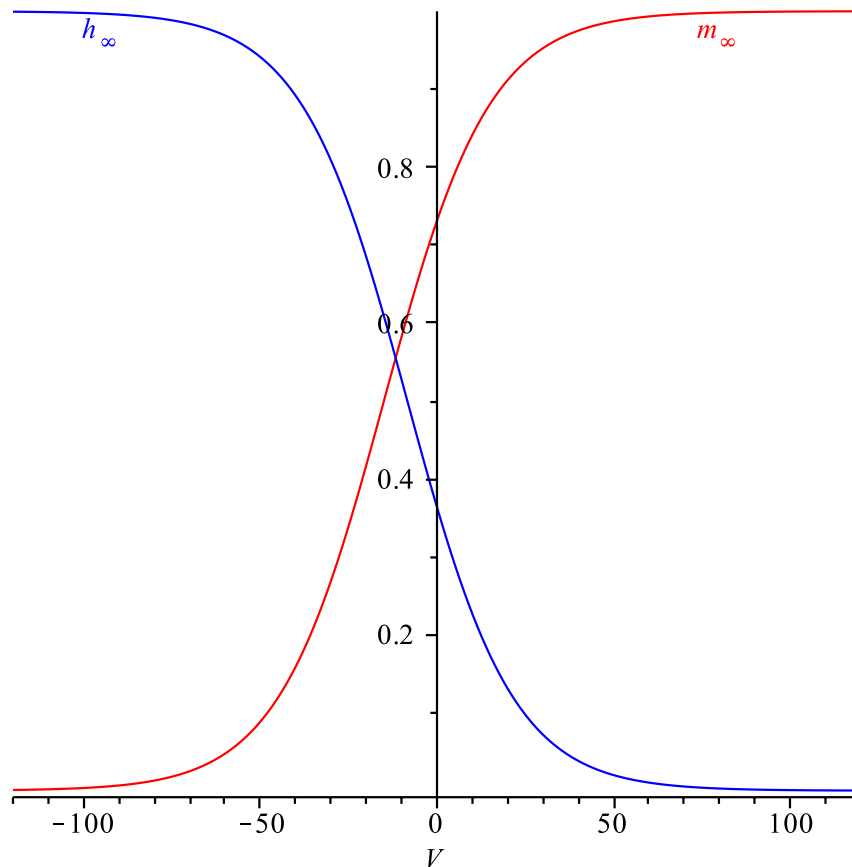
Figure 4.1: Example $m_\infty(V)$ and $h_\infty(V)$

4.3   General Method

We will describe the general method for fitting parameters to the equations described above. We start by writing out a general form of the equation for which we are trying to fit parameters

$$I_i = \bar{g}_i m_i(V)^p h_i(V)(V - E_i) \tag{4.9}$$

This is valid for voltage dependent currents. The calcium dependent components of channels as well as calcium dynamics will be described in later sections devoted to those specific

topics. Note that the section is split into activation and inactivation subsections, but in the activation section we will be focusing on data when the inactivation variable is assumed to be approximately 1 and thus the procedure applies to currents with no inactivation variable. Any differences from the general method due to availability of data will also be described in a section addressing the specific current.

4.3.1 Activation Steady State

We will be using the steady state and time constant differential equations seen below to model the activation variable for the currents in the Aplysia bag-cell neuron.

$$\frac{\mathrm{d}m}{\mathrm{d}t} = \frac{m_\infty(V) - m}{\tau_m(V)} \tag{4.10}$$

$$m_\infty(V) = \frac{1}{(1 + e^{\frac{V - V_m}{K_m}})^p} \tag{4.11}$$

$$\tau_m(V) = \tau_{m0} \frac{e^{\frac{\delta_m(V - V_m)}{K_m}}}{1 + e^{\frac{(V - V_m)}{K_m}}} \tag{4.12}$$

These equation give us four parameters to fit: V_m, K_m, δ_m, and τ_{m0}. Additionally we will also determine $\bar{g}_i$ from Equation (4.9) using the same data we use for $m_\infty(V)$. In order to fit parameters for the steady state activation function, $m_\infty(V)$, we use data from voltage clamp experiments done where only a single current is expressed. For an example of what the resulting data from a voltage clamp experiment (as discussed in Section 2.2.3) looks like see Figure 4.2. We denote the pre-clamp holding voltage V_{pre} and the holding voltage will be V. To describe the fitting method we will use an arbitrary current I_i. We start by using the differential equations for the activation variable m and inactivation variable h and solving with the assumption that at the initial time $t = 0$ and $V = V_{pre}$. Solving Equation (4.10) to gives us

$$m(t) = m_\infty(V) + (m_\infty(V_{pre}) - m_\infty(V))e^{-\frac{t}{\tau_m}} \tag{4.13}$$

and similarly we can solve

$$\frac{\mathrm{d}h}{\mathrm{d}t} = \frac{h_\infty(V) - h}{\tau_h(V)} \tag{4.14}$$

to obtain

$$h(t) = h_\infty(V) + (h_\infty(V_{pre}) - h_\infty(V))e^{-\frac{t}{\tau_h}} \tag{4.15}$$

We can combine these results with Equation (4.9) to get an expanded current equation
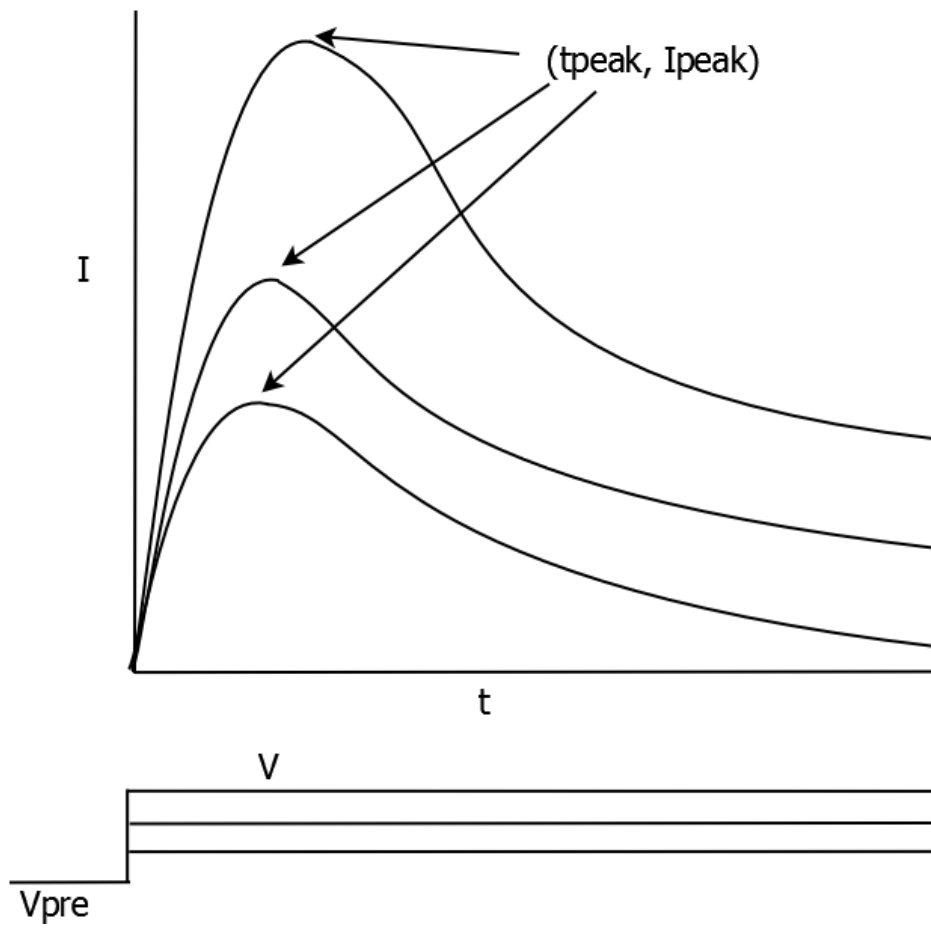
Figure 4.2: Voltage Clamp Example

$$I_i = \bar{g}_i(V - E_{ion})[m_\infty(V) + (m_\infty(V_{pre}) - m_\infty(V))e^{-\frac{t}{\tau_m}}]^p[h_\infty(V) + (h_\infty(V_{pre}) - h_\infty(V))e^{-\frac{t}{\tau_h}}] \quad (4.16)$$

Let $(t_{peak}, I_{i,peak})$ be the peak of the current versus time curve in the voltage clamp experiment, see Figure 4.2. At this point we assume the inactivation has not yet started, i.e. that $t_{peak} << \tau_h$ which implies $e^{-\frac{t_{peak}}{\tau_h}} \approx 1$. With this assumption we can simplify Equation (4.16) to

$$I_{i,peak}(V) = I_i(t_{peak}) = \bar{g}_i(V - E_{ion})[m_\infty(V) + (m_\infty(V_{pre}) - m_\infty(V))e^{-\frac{t_{peak}}{\tau_m}}]^p[h_\infty(V_{pre})] \quad (4.17)$$

We further assume that the current is fully activated, i.e., $\tau_m << t_{peak}$ which implies $e^{-\frac{t_{peak}}{\tau_m}} \approx 0$. We then obtain an equation for conductance as a function of V

$$G_i = \frac{I_{i,peak}(V)}{V - E_{ion}} \quad (4.18)$$

$$G_i = \bar{g}_i m_\infty(V)^p h_\infty(V_{pre}) \quad (4.19)$$

We further assume that $h_\infty(V_{pre}) \approx 1$ since V_{pre} is negative enough for there the inactivation variable to be 1. Generally at membrane potentials significantly below the rest potential the activation variable m is near 0 and the inactivation variable is 1 due to the sigmoidal shape of their steady state curves which represents the channel being closed. Thus for voltage clamp experiments the pre-pulse value is set negative enough for $h_\infty(V_{pre}) \approx 1$ to be a good approximation. Note that this simplification brings us to the same equation we would have had for a current with no inactivation variable. The conductance equation now becomes

$$G_i(V) = \bar{g}_i m_\infty(V)^p \quad (4.20)$$

where $m_\infty(V)$ is of the form seen in Equation (4.5) and thus we have

$$G_i(V) = \frac{\bar{g}_i}{(1 + e^{\frac{V - V_m}{K_m}})^p} \quad (4.21)$$

In order to fit these parameters we convert the peak current values into conductance values using Equation (4.18). We either extract the values of I_{peak} from the voltage clamp experiments plot using a digitizer or extract the data from a peak current versus membrane potential plot which is commonly included with voltage clamp experimental data. The peak current versus voltage plot is referred to as an I-V curve. To fit the parameters we use a

Matlab nonlinear least squares curve-fitting algorithm (the function *lsqcurvefit*) to determine the values of $\bar{g}_i$, V_m, and K for integer values of p from 1 to 4 and determine the best fit.

The Matlab function *lsqcurvefit* solves nonlinear curve-fitting problems in a least squares sense. The algorithm was used with four inputs, the x-axis data, the y-axis data, the function to be fitted and the initial condition of the parameters to be fitted. Upper and lower bounds can be specified for the value of each parameter but for our purposes that often leads to the algorithm simply stopping at the boundary. However it is not difficult to pick good starting conditions for the sigmoidal functions due to the simple relationship between the parameter values and the shape of the function previously discussed. We will report all results of *lsqcurvefit* with an error value. The error value is the squared 2-norm of the residual at V, i.e. $\sum((fitfunction(params, V) - Idata)^2)$

4.3.2   Activation Time Constant

Next we want to fit the parameters of $\tau_m(V)$. First we take $t_{\frac{1}{2}}$ to be the time such that $I_i(t_{\frac{1}{2}}) = \frac{I_{peak}}{2}$. Then Equation (4.17) becomes

$$I_i(t_{\frac{1}{2}}) = \bar{g}_i(V - E_{ion})[m_\infty(V) + (m_\infty(V_{pre}) - m_\infty(V))e^{-\frac{t_{\frac{1}{2}}}{\tau_m}}]^p h_\infty(V_{pre}) \tag{4.22}$$

For convenience in further calculations we let

$$M = \frac{m_\infty(V_{pre})}{m_\infty(V)} \tag{4.23}$$

and then if we divide Equation (4.22) by Equation (4.17) we have

$$
\begin{aligned}
\frac{1}{2} &= \frac{I_{i,1/2}}{I_{i,peak}} \\
&= \frac{[m_\infty(V) + (m_\infty(V_{pre}) - m_\infty(V))e^{-\frac{t_{\frac{1}{2}}}{\tau_m}}]^p}{[m_\infty(V) + (m_\infty(V_{pre}) - m_\infty(V))e^{-\frac{t_{peak}}{\tau_m}}]^p} \\
&= \frac{[1 + (M - 1)e^{-\frac{t_{1/2}}{\tau_m}}]^p}{[1 + (M - 1)e^{-\frac{t_{peak}}{\tau_m}}]^p} \tag{4.24}
\end{aligned}
$$

This can be rearranged as follows

$$\frac{1}{2}[1 + (M - 1)e^{-\frac{t_{peak}}{\tau_m}}]^p - [1 + (M - 1)e^{-\frac{t_{1/2}}{\tau_m}}]^p = 0 \tag{4.25}$$

34

and then solved for $\tau_m(V)$ assuming we know $m_\infty(V)$. However if we make the assumption that $m_\infty(V_{pre}) \approx 0$, i.e. that the pre-pulse potential was low enough that there is no activation, we have $M = 0$. Equation (4.25) then becomes

$$\frac{1}{2}[1 - e^{-\frac{t_{peak}}{\tau_m}}]^p - [1 - e^{-\frac{t_{1/2}}{\tau_m}}]^p = 0 \tag{4.26}$$

We also assume that that $t_{peak} >> \tau_m$ which implies $e^{-\frac{t_{peak}}{\tau_m}} \approx 0$ which greatly simplifies Equation (4.25) giving

$$\frac{1}{2} - (1 - e^{-\frac{t_{1/2}}{\tau_m}})^p = 0 \tag{4.27}$$

which we can solve for $\tau_m(V)$ to get the following equation

$$\tau_m(V) = -\frac{t_{\frac{1}{2}}}{ln((1 - (\frac{1}{2})^{\frac{1}{p}}))} \tag{4.28}$$

Using the data in figures we can convert the $t_{\frac{1}{2}}$ values to $\tau_m(V)$ using the equation above. We can then fit parameters τ_0 and δ using *lsqcurvefit* method in Matlab.

4.3.3   Inactivation

In order to find the parameters for $h_\infty(V)$ and $\tau_h(V)$ we start with the expanded form of Equation (4.16) as we did for the activation parameter fitting. We take

$$I_i = \bar{g}_i(V - E_i)[m_\infty(V) + (m_\infty(V_{pre}) - m_\infty(V))e^{-\frac{t}{\tau_m}}]^p[h_\infty(V) + (h_\infty(V_{pre}) - h_\infty(V))e^{-\frac{t}{\tau_h}}]$$

and we take experimental data from the voltage clamp experiment for which t is large, i.e. t is significantly greater than t_{peak}. Thus we can assume that $m(V) = m_\infty(V)$, which we have already found. Then the current equation becomes

$$I_i = \bar{g}_i(V - E_i)[m_\infty(V)]^p[h_\infty(V) + (h_\infty(V_{pre}) - h_\infty(V))e^{-\frac{t}{\tau_h}}] \tag{4.29}$$

which is equivalent to

$$I_i(V) = A_1(V) + A_2(V)e^{-\frac{t}{\tau_h}} \tag{4.30}$$

where

$$A_1(V) = \bar{g}_i(V - E_i)[m_\infty(V)]^p h_\infty(V) \tag{4.31}$$
$$A_2(V) = \bar{g}_i(V - E_i)[m_\infty(V)]^p[(h(V_{pre}) - h_\infty(V))] \tag{4.32}$$

We use Matlab to fit Equation (4.30) to the inactivating section of the voltage clamp curves for different values of V. This explicitly gives us data for $\tau_h(V)$ and we can solve $A_1(V)$ to determine $h_\infty(V)$ by rearranging the above equation to get

$$h_\infty(V) = \frac{A_1(V)}{\bar{g}_i(V - E_i)[m_\infty(V)]^p} \tag{4.33}$$

We now have data for both $\tau_h(V)$ and $h_\infty(V)$ and we use Matlab to fit parameters as we did for the activation functions.

4.3.4   Voltage Clamp Simulation

We make more adjustments to the parameters by simulating the voltage clamp experiments which were the source of the data. To create these simulations we use XPPAUT. XPPAUT is a numerical ordinary differential equation simulator created by Dr. Bard Ermentrout of the University of Pittsburgh which includes the bifurcation package AUTO. The simulations for our system of differential equations were done using the Runge Kutta fourth order method with step size 0.05 msec.

4.4   Currents

4.4.1 I_A

I_A is the transient outward current that is responsible for shaping the spiking frequency and serves to prevent action potential initiation at hyperpolarized potentials.

The experimental data for the A-current comes from Strong [31]. Strong carried out a voltage clamp experiment where the cell was held at -95 mV in order to ensure there was no inactivation, the cell was then stepped up to values between -55 mV and -15 mV. The results are shown in Figure 2B of [31]. Figure 2C is the accompanying I-V curve which shows the peak current value for each potential at which the cell was held. Using a digitizer we extracted the values from Figure 2C and then converted the current values to conductance as described in Section 4.3. The Nernst potential for potassium was determined to be -80 mV from the zero of the I-V curves of the inward potassium channels. The voltage clamp experiment gives us 9 points of data.
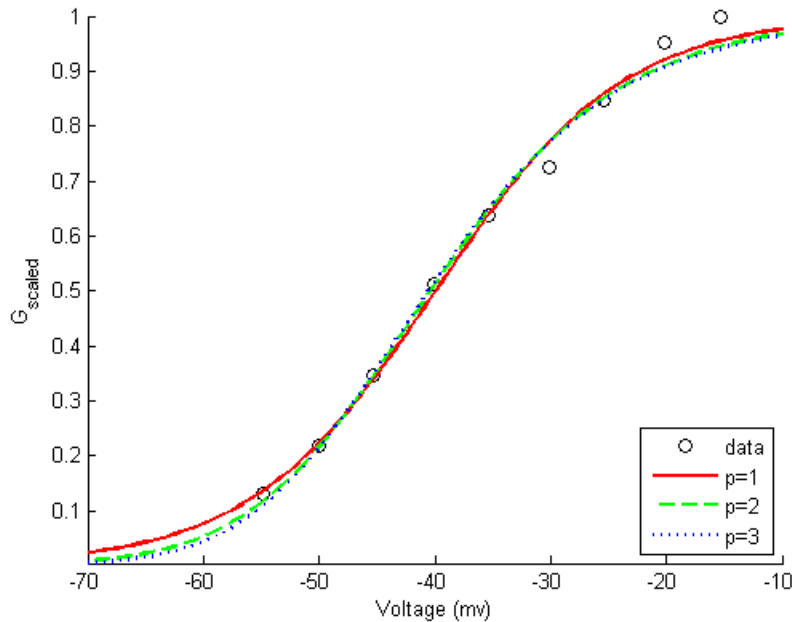
Figure 4.3: $m_{\infty A}(V)$ fits for various values of p

We tried fitting a function of the form of the Equation (4.21) for different values of p but the *lsqcurvefit* algorithm converged to a value a maximum conductance value that did not make physical sense. We set $\bar{g}_A$ to 0.1653 which is the maximum conductance value from the data and fit V_m and K_m. The results are shown in table 4.1 and Figure 4.3.

Table 4.1: Parameter Values for Activation of I_A

p	V_m	K_m	error
1	-39.9174	-8.0696	0.0057
2	-48.6597	-9.4135	0.0072
3	-53.9542	-9.9590	0.0083

Next we fit $\tau_{mA}(V)$ to the form of Equation (4.8) using Figure 12A which plots the time to half-peak versus membrane holding potential and is shown in Figure 2B. Using the data in figures 12A we converted the half peak times, $t_{\frac{1}{2}}$, to $\tau_{mA}(V)$ using Equation (4.28). We fit parameters τ_0 and δ using *lsqcurvefit* in Matlab as before. The resulting parameter fits can be seen in Table 4.4.1 and Figure 4.4.1.

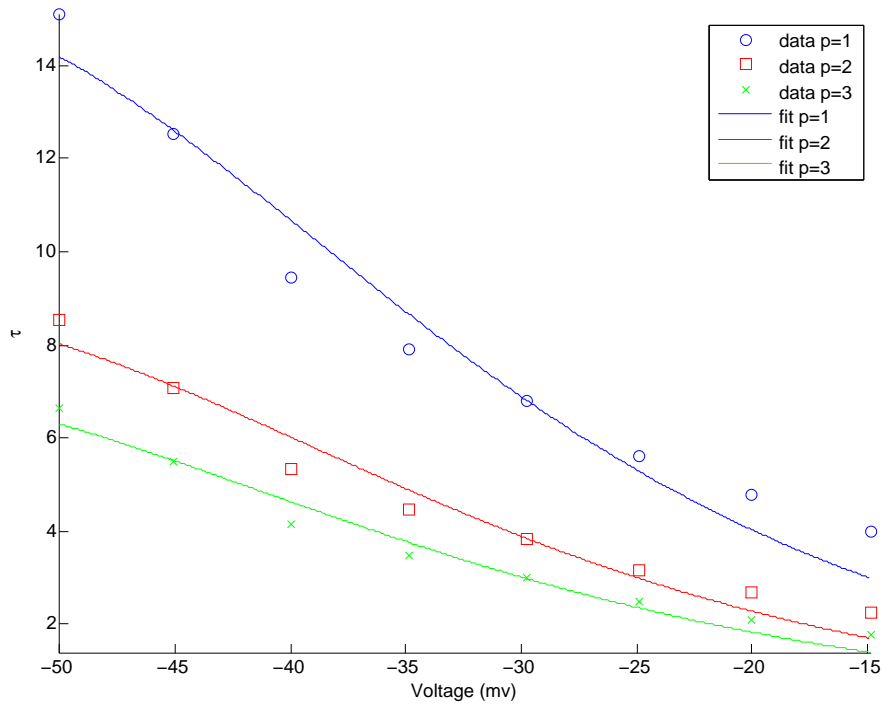| p	τ_0	δ	error	scaled error
1	28.1645	0.2436	4.6524	0.0203
2	16.6969	0.2806	1.4389	0.0197
3	13.8690	0.3827	0.6476	0.0147

Figure 4.4: $\tau_{mA}(V)$ fit for I_A

Since different p values produce different $\tau_{mA}(V)$, the error of comparing the residual needs to be adjusted to account for the different y-axis scales. We do this scaling by dividing the error for each fit by the square of the maximum value of $\tau_{mA}(V)$ for that value of p. The differences between fits for different values of p are insignificant when comparing the scaled errors. Since all the fits are good we chose p to be 1 as it provides the simplest formula.

In Strong's 1984 paper [31] the $h_\infty(V)$ inactivation data is provided and fit a function of the form seen in Equation (4.5). The constants were determined to be $K_{h_A} = 4.7$ and $V_{h_A} = -82.4$. Using the same data points as Strong we confirmed the parameters are a good fit.

Next we fit $\tau_{hA}(V)$ to a function of the form of Equation (4.8). For the $\tau_{hA}(V)$ data we used Figure 10 of [31] which provides data for $\tau_{hA}(V)$ for different membrane potentials. The $\tau_{hA}(V)$ value was determined by fitting an exponential to the tail end of the voltage clamp experiments. We ran the fitting process twice because the first fit did not provide accurate results for V greater than -50 mV. We adjusted our fit by removing the points less than -50 mV.

Voltage Clamp Simulation

We replaced τ_h with a constant value of 125 since the fit levelled off at roughly that value and the bell shaped section of the curve occurs mostly at voltages below the cell's normal activity range. In recreating the voltage clamp experiments from Figure 2B we found that $\tau_m(V)$ needed to be very small as the activation of I_A is almost instantaneous. We also increased the conductance, $\bar{g}_A$ to 0.36 to have a peak value similar to the voltage clamp experiments from which the data was taken. The fit is shown in Figure 4.5.

4.4.2 I_{K1}

I_{K1} is a voltage dependent potassium channel which has only an activation component. The role of I_{K1} is to repolarize the action potential and regulate the width of the action potential.

All data is from Quattrocki et al.'s 1994 paper ([27]). I_{K1} has no inactivation so we model it with the following equation

$$I_{K1} = \bar{g}_{K1} n_{K1}^p (V - E_K) \tag{4.34}$$

where $n_{K1}(V)$ is modelled as before for an activation variable. The data for $n_{\infty K1}(V)$ was taken from Figure 4D in Quattrocki. Figure 4D is a peak current versus membrane potential plot. The peak current is taken from a voltage clamp experiment where a cell that strongly expresses I_{K1} was held at -60 mV and stepped to potentials ranging from -40 mV to +30 mV. The voltage clamp results are shown in Figure 4B of [27]. The data from 4D gives us the peak current value scaled by the maximum peak current value, specifically $\frac{I_{peak}(V)}{I_{peak}(30)}$. We
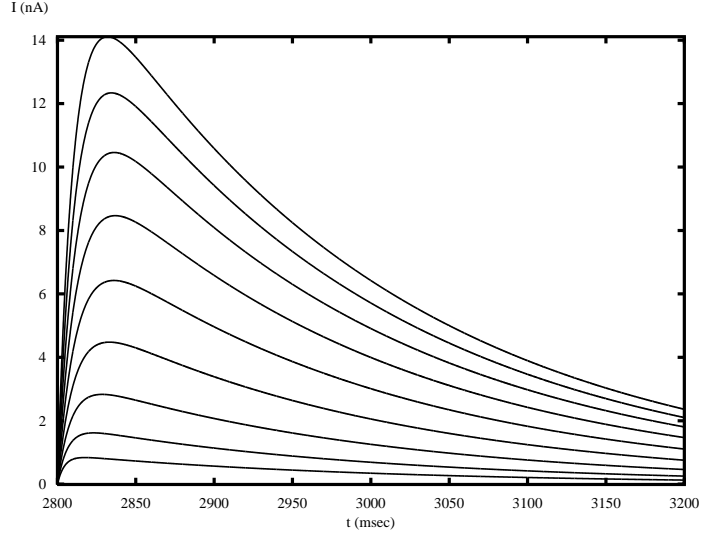
Figure 4.5: Voltage Clamp for I_A

extracted $I_{peak}(30)$ from Figure 4B and used it to determine $I_{peak}(V)$ for other membrane potentials. Once we had the data for $I_{peak}(V)$ we calculated the conductance values, $G_{K1}(V)$, using Equation (4.18). The results are shown in Table 4.2 and Figure 4.7

Table 4.2: Activation Parameters for I_{K1}

P	$\bar{g}_{K1}$	V_n	K_n	error
1	0.0659	-33.2331	19.9529	0.00001455
2	0.0669	-52.9587	22.9508	0.00001232
3	0.0672	-64.9873	24.0465	0.000011163

Next we fit $\tau_{nK1}(V)$ by taking the time to half maximum from the voltage clamp in Figure 4B and then calculating $\tau_{nK1}(V)$ for each p value using Equation (4.28) and fitting a function as before. The time to half maximum values were determined by using a digitizer to extract the peak value and then finding the point on the curve that was half the peak value. The fit is shown in Table 4.3 and Figure 4.8.

Table 4.3: τ_{nK1} Parameter Fits

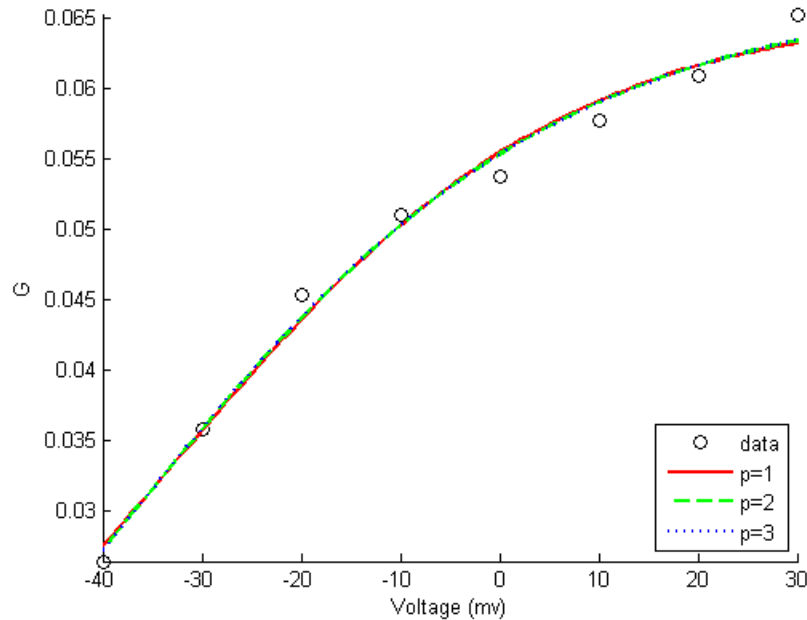| P	τ_{0K1}	δ_{K1}	scaled error
1	92.5662	0.0901	0.0317
2	76.6947	0.1501	0.0996
3	75.5775	0.1772	0.1646

40

Figure 4.6: $n_{\infty K1}$ fit for I_{K1}

Figure 4.7: I_{K1} activation variable fit

Voltage clamp Simulation

Simulation of voltage clamp experiments from Quattrocki ([27]) are shown in Figure 4.9. The simulation is a very good match to the actual voltage clamp experiment.

4.4.3 I_{K2}

I_{K2} is a voltage gated outward potassium current with both activation and inactivation components. Like I_{K1} the current is responsible for spike broadening and repolarization of the membrane potential during an action potential.

Activation

The activation data for I_{K2} was taken from Quattrocki et al. 1994 [27] Figure 4D and 4A. Figure 4D is the same as used for I_{K1} and also contains peak current versus membrane potential data for I_{K2}. Figure 4A contains a voltage clamp experiment for I_{K2} where the cell was held at -60 mV and stepped up to holding voltages from -40 mV to +40 mV. As with I_{K1} we found a normalized $I_{peak}(V)$ from Figure 4D and then multiplied by $I_{peak}(40)$ to get $I_{peak}(V)$ values. We then converted $I_{peak}(V)$ from current to conductance as before
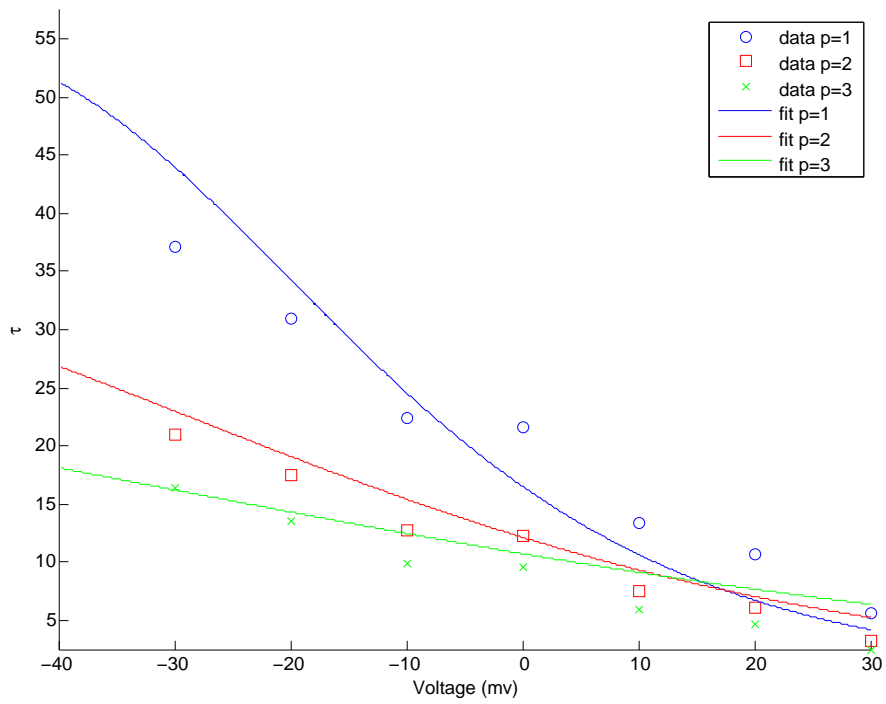
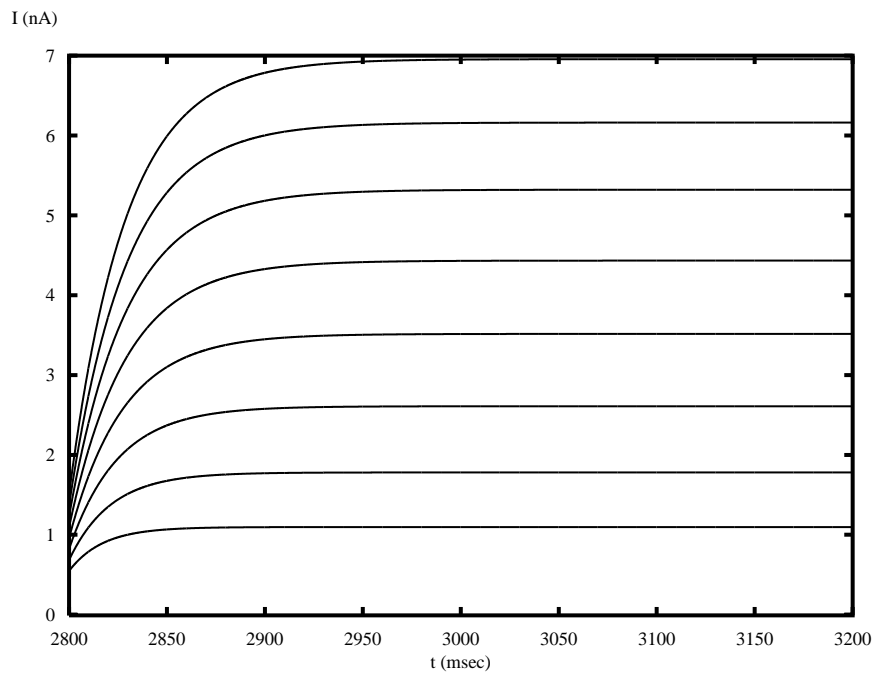Figure 4.8: τ_{nK1} fit for I_{K1}
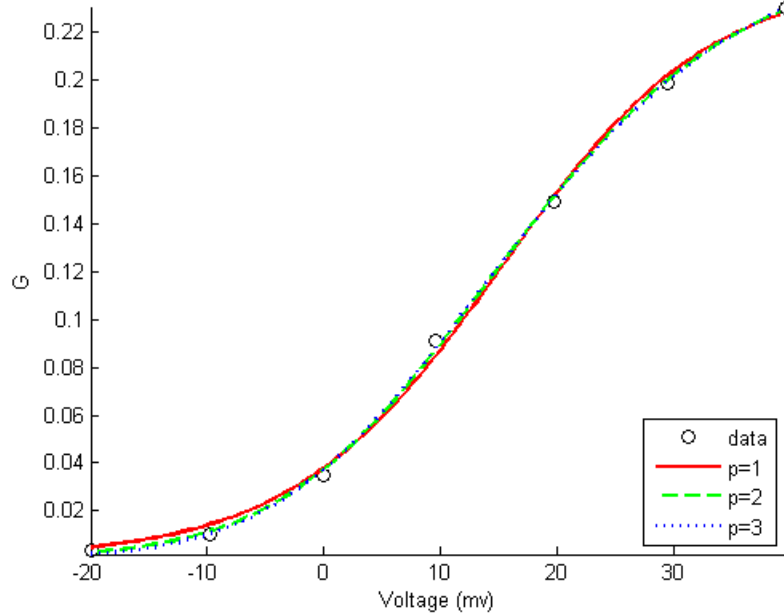
Figure 4.9: Voltage Clamp for I_{K1}

Figure 4.10: $m_{\infty K2}(V)$ fits for various values of p

using Equation (4.18). We then fit the parameters of $m_\infty(V)$ using the *lsqcurvefit* function in Matlab. The results are shown in the Table 4.5 below and Figure 4.10.

Table 4.4: I_{K2} Parameter Fit

P	$\bar{g}_{K2}$	V_{mK2}	K_{mK2}	$error$
1	0.2435	15.053	-8.9191	0.00001625
2	0.2557	5.4067	-11.4679	0.00000707
3	0.2619	-1.033	-12.6744	0.00000546

For $\tau_{mK2}(V)$ we took the time to half-maximum values from the voltage clamp shown in Figure 4A and transformed the values $\tau_{mK2}(V)$ as before. We then fit the parameters to Equation (4.8) for different values of p. However there was not enough data to get a reasonable fit and due to the steepness of the initial rise of the current in the voltage clamp experiments it was very difficult to accurately determine the time to half maximum. Instead we used a constant for $\tau_{mK2}(V)$ which was fit by simulating the voltage clamp experiments and adjusting the parameter so the simulation matched the actual experiment.

Inactivation

We used Figure 3B to determine the values for $h_{\infty K2}(V)$. Figure 3B plots steady state inactivation against membrane potential. The steady state inactivation is determined by

holding the cell at -80 mV then stepping the potential up to a prepulse potential between -80 mV and 10 mV in 10 mV increments. After being held at the prepulse potential for 1.5 seconds to let the inactivation go to steady state, the cell is clamped at 20 mV to elicit the remaining current. The peak of the remaining current was normalized and plotted against the prepulse voltage. The $h_{\infty K2}(V)$ fit is shown in Figure 4.11

Table 4.5: I_{K2} Parameter Fit

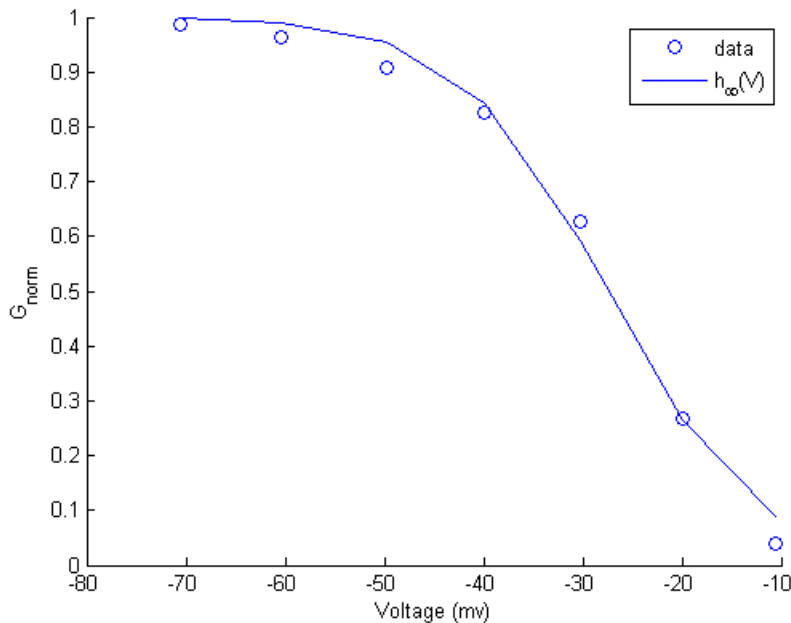| V_h	K_h	error
-27.5467	-7.3401	0.0071

Figure 4.11: $h_{\infty K2}(V)$ parameter fit results

Next we use the general method described in Section 4.3 to fit a curve of the form $I_{K2} = A_1(V) + A_2(V)e^{-\frac{t}{\tau_h}}$ to the last 200 msec of the voltage clamp data from Figure 4A. This gives us 5 data points for τ_h which is an insufficient range of membrane potentials to fit a bell shaped curve. These results are shown in Table 4.6 below.

We take τ_h to be the average of the points in Table 4.6, 88.7305.

Voltage Clamp Simulation

The fit is shown in Figure 4.12, the only changes that were made were a slight increase in the maximum conductance to 0.12 to account for the fact the inactivation variable is not 1 at the peak values of the current. We adjusted the value of $\tau_{mK2}(V)$ to be 9 to match the voltage clamp experiment data.

45

Table 4.6: τ_h Data

V	τ_h
0	93.9162
10	84.8528
20	79.0492
30	82.1083
40	103.726

I (nA)
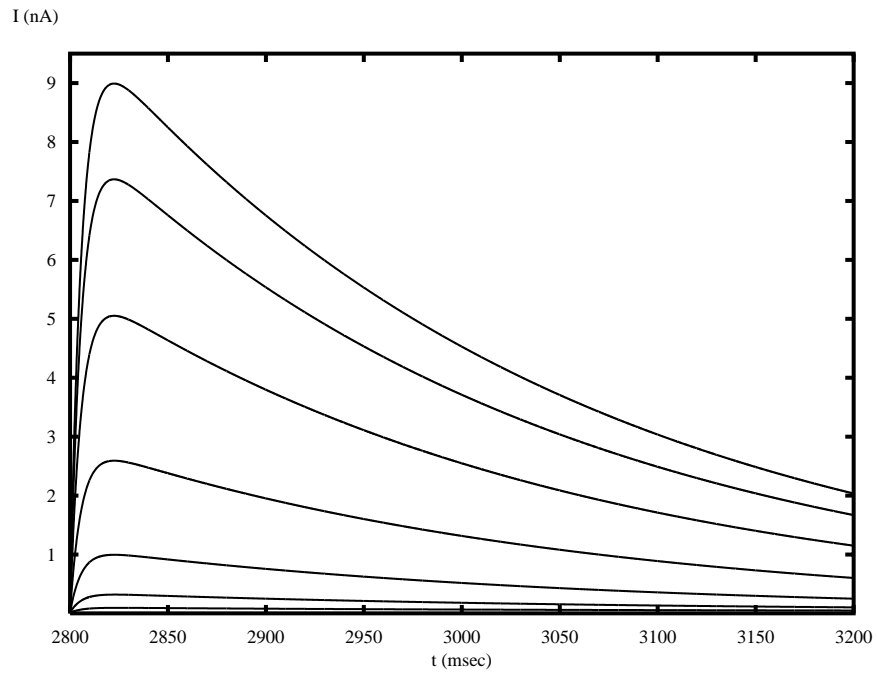
Figure 4.12: Voltage Clamp for I_{K2}

Table 4.7: I_{Ca} Parameter Values

P	$\bar{g}_{Ca}$	V_m	K_m	error
1	0.1168	-3.3863	5.7564	0.0003043
2	0.1173	-9.7085	6.8655	0.0003347
3	0.1172	13.4379	19.5559	0.0003518

4.4.4 $\mathbf{I_{Ca}}$

I_{Ca} is an inward current carried by calcium which is responsible for the upstroke portion of the action potential. It is the only current in the model that causes an increase in membrane potential. The calcium current exhibits a use-dependent inactivation which is partially responsible for the spike broadening during a spike train.

Activation

In order to model I_{Ca}, first we found E_{Ca} using the right side of the I-V curve found in Figure 5A from [8]. We determined E_{Ca} by using the data in the I-V curve to solve for $I(E_{ca}) = 0$. We did this by fitting a polynomial curve to the data and then solving the fitted curve for $I(E_{Ca}) = 0$. We used only the data after the minimum to get a better fit since for this current the I-V graph forms and upside-down bell shaped curve. We used a quadratic fit to determine $E_{Ca} = 57.5699$ with an error of 0.00778.

Next we used the same method as previous currents to fit $m_\infty(V)$ using the peak current versus membrane potential plot in Figure 5 of [8]. Figure 5 is a voltage clamp experiment where the cell was held at -60 mV and stepped in 10 mV increments from -60 mV to +60 mV.

The errors for each fit are so small that there is no significant difference between fits, we take p to be 1 for simplicity.

Next we fit τ_m using Figure 2B from Zhang [37] and starting out by fitting a curve of the form $I_{Ca} = A_1(V) + A_2(V)e^{-\frac{t}{\tau_m}}$ to the activating section of the voltage clamp curves. This is similar to the method described in the inactivation section of the general method and follows from Equation (4.16). The activation section occurs for roughly the first 30 milliseconds until the current reaches its peak, afterwards the assumption that $h \approx 1$ is no longer valid. The results can be seen in Table 4.8

As before we fit this data to the function of seen in Equation (4.8) with results of $\delta_{mCa} = 0.1773$ and $\tau_{0mCa} = 8.5538$, but the error for this was 23.6548. The error was too large so instead we tried fitting a simple decaying exponential of the form $Ae^{-\frac{V}{B}}$. The result was A=3.3308 and B=83.2560 with the error of 0.5680. However, we lack data for voltages less than -30 mV, so we have no way of fitting a curve that accurately represents values of $\tau_{mCa}(V)$ for low membrane potentials. However since I_{Ca} is not active until quite depolarized values we use the fit in our model.
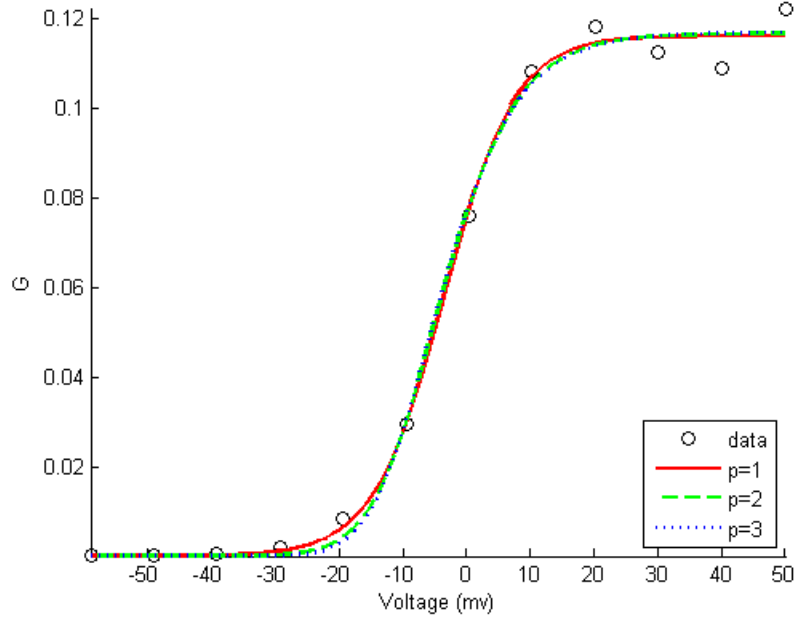
Figure 4.13: $m_{\infty Ca}(V)$ fit

Table 4.8: τ_{mCa} Values

V	τ_{mCa}	error
-30	4.7309	0.0036
-20	4.2563	0.0053
-10	4.0346	0.0022
0	3.1781	0.2598
10	3.0937	0.6747
20	2.1527	0.6720
30	2.0478	0.3611
40	2.3745	0.0362
50	2.0397	0.0028

Inactivation

We use the general method with data taken from the voltage clamp experiment shown in Figure 5 of Hung and Magoski [15] to fit parameters for $h_{\infty Ca}(V)$ and $\tau_{hCa}(V)$. The results are shown in Tables 4.9 and 4.10

Table 4.9: $h_{\infty Ca}(V)$ Parameters

P	V_h	K_h	error
1	28.0559	-15.5973	0.0539

Table 4.10: τ_{hCa} Data

V	τ_{hCa}
-20	71.8911
-10	63.3692
0	64.8659
10	66.2832
20	64.8080
30	64.5052
40	132.8472
50	71.3100

However the values in Table 4.10 did not provide adequate parameter fits for the usual function, instead we took the average value of the data without the outlier of 132.8472 to get a $\tau_{hCa}(V)$ value of 65.83.

Use-Dependent Inactivation

In Figure 6d of Hung and Magoski [15] the calcium current exhibits use-dependent inactivation during repeated voltage clamp experiments. Without a specific mechanism known to cause the use-dependent inactivation we decided to use the internal calcium level as seen in various calcium dependent currents seen and discussed in Chapter 11 of Voltage-Gated Calcium Channels [23]. We will discuss the internal calcium dynamics in Section 4.4.6, for now we will just look at the effects of calcium concentration on I_{Ca}. We incorporated the calcium into the inactivation variable, h. More specifically we chose to have calcium decrease the rate at which the channel opens, $\alpha_{hCa}(V)$. The rate at which channels close is modelled by the variable $\beta_{hCa}(V)$, where $\alpha_{hCa}(V)$ and $\beta_{hCa}(V)$ relate to $h_{\infty Ca}(V)$ and $\tau_{hCa}(V)$ as follows

$$h_{\infty Ca}(V) = \frac{\alpha_{hCa}(V)}{\alpha_{hCa}(V) + \beta_{hCa}(V)} \tag{4.35}$$

49

$$\tau_{hCa}(V) = \frac{1}{\alpha_{hCa}(V) + \beta_{hCa}(V)} \tag{4.36}$$

and $\alpha_{hCa}(V)$ and $\beta_{hCa}(V)$ are taken to be the following functions from Willms 1999 paper [34]

$$\alpha_{hCa}(V) = a_0 e^{\frac{-\delta V}{s}}$$

$$\beta_{hCa}(V) = b_0 e^{\frac{(1-\delta)V}{s}} \text{ where } 0 \le \delta \le 1$$

The observed behaviour , that $h_{\infty Ca}(V)$ increases as [Ca] could be obtained by modifying either $\alpha_{hCa}(V)$ or $\beta_{hCa}(V)$ to be calcium dependent. However we chose to modify $\alpha_{hCa}(V)$ to be a function of V and calcium concentration by having an increase in calcium cause a decrease in $\alpha_{hCa}(V)$. We chose $\alpha_{hCa}(V)$ rather than $\beta_{hCa}(V)$ because a decrease in $\alpha_{hCa}(V)$ causes a decrease in $h_\infty(V)$ and an increase in $\tau_{hCa}(V)$, which agrees with behaviour observed by Magoski et al. [15] that in the absence of calcium (barium replaced calcium in the experiment) it was found that I_{Ca} inactivated faster, i.e., $\tau_{hCa}(V)$ was larger.

The calcium dependence was inserted as follows

$\alpha_{hCa}(V, Ca) = \frac{a_0}{F(Ca)} e^{\frac{-\delta V}{s}}$ where F(Ca) is some function of calcium to be determined. We substitute $\alpha_{hCa}(V, Ca)$ and $\beta_{hCa}(V)$ into Equation (4.35) and rearrange to get

$$h_\infty(V) = \frac{1}{1 + \frac{b_0 F(Ca)}{a_0} e^{\frac{V}{s}}} \tag{4.37}$$

which can be put in the form of a Boltzmann function similar to Equation (4.11) but with p equal to 1, by choosing $V_{hCa} = -s \ln(\frac{b_0 F(Ca)}{a_0})$. We choose F(Ca) so that at the resting value of internal calcium concentration we have the same value for V_{ha} as previously determined. Thus we can simplify our equation for V_{hCa} and put it in terms of parameters we have already calculated which yields

$$V_{hCa} = V_h - K \ln(F(Ca)$$

and we chose F(Ca) as follows

$$F(Ca) = (1 + (Ca - Ca_{Rest}))$$

Since our inactivation time constant for I_{Ca} is actually a constant value rather than dependent on V, we do not actually model any effect of calcium on the rate of inactivation of I_{Ca}. The calcium dependence we introduced has the effect of shifting the inactivation steady state curve to the left each time the calcium level increases thus causing the calcium current to inactivate at a lower membrane potential with repeated use.

Voltage Clamp Simulation

Since the current is now partially inactivated to due voltage and partially due to calcium levels, we had to adjust our $\tau_{hCa}(V)$ parameter. Once again we altered $\tau_{hCa}(V)$ to get the proper qualitative behaviour over long time spans, we increased the value to 300. The simulation of Figure 5a from Magoski et al. [15] is shown in Figure 4.14.
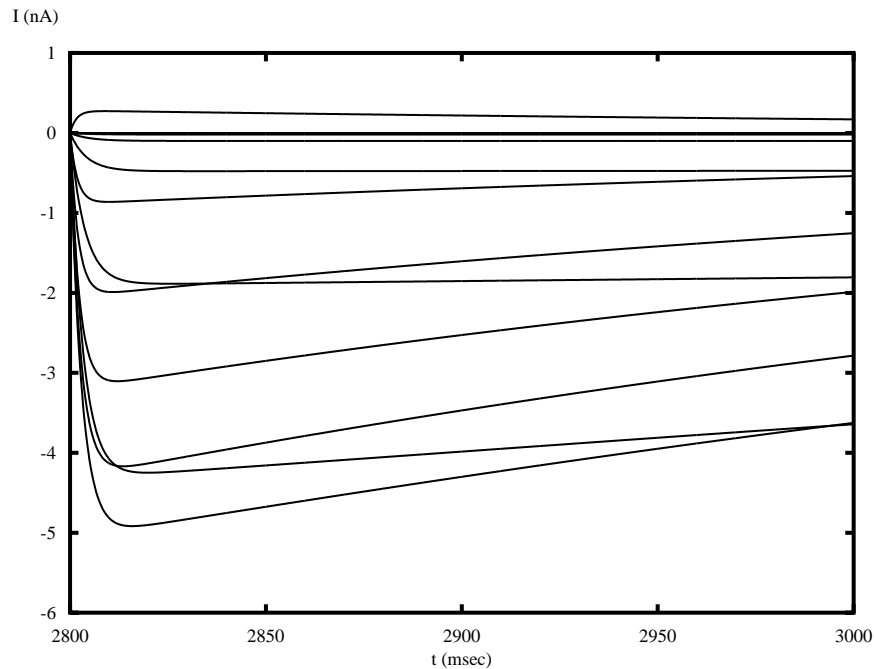

Figure 4.14: Voltage Clamp for I_{Ca}

4.4.5 I_{KC}

Current Description

I_{KC} is the calcium dependent potassium current. It is both voltage and calcium activated with no inactivation.

Voltage Dependent Activation

We begin by ignoring the calcium dependence and fitting a normal activation gating variable similar to I_{K1}

First we used Figure 2B from Zhang et al. [36], which shows an I-V curve for the I_{KC} channels that have been cloned and expressed in oocytes. This means we cannot use the data to determine the maximum conductance, $\bar{g}_{KC}$. Instead we have

$$\hat{G}(V) = \frac{\hat{I}_{KC,peak}(V)}{V - E_K} = \hat{g}_{KC}[n_\infty]^p \tag{4.38}$$

where $\hat{g}_{KC}$ is not the true conductance value of the channel since it is taken from gene expression data. The results were as follows

P	$\bar{g}_{KC}$	V_n	K_n	error
1	0.0784	32.0191	21.7066	0.00004232
2	0.0811	8.3680	27.7566	0.0000020444
3	0.0824	-7.7632	30.5101	0.0000014247
4	0.0831	-19.6994	32.0344	0.0000011466

Once again the differences in the errors for each fit are insignificant so we used p equal to 1 for simplicity.

Next we used Figure 2A of Zhang [37]. Figure 2A shows a voltage clamp experiment measuring potassium current before and after the application of a drug the specifically blocks the type of calcium activated potassium current we are modelling. The plot also shows the difference between the control and blocked voltage clamp currents which represents I_{KC}. We used the difference currents to find the maximum value of I_{KC}. We then calculated $\bar{g}_{KC}$ from $\hat{g}_{KC}$ using the following formula derived below

We combine

$$I_{KC} = \bar{g}_{KC}(60 - E_K)n^p$$

and

$$\hat{I}_{KC} = \hat{g}_{KC}(60 - E_K)n^p$$

to get

$$\bar{g}_{KC} = \hat{g}_{KC}\frac{I_{KC,peak}(60)}{\hat{I}_{KC}} \tag{4.39}$$

which gave us a value of 0.0589 for $\bar{g}_{KC}$, where $\hat{I}_{KC}(60)$ was taken from Zhang [36] Figure 2B and I_{KC} was taken from Figure 2A mentioned above.

Next we tried using the difference current inset from Zhang [37] to find $\tau_{mKC}(V)$ but could not get accurate enough results due to the small size of the figure.

Calcium Dependence

We modelled the Calcium dependence as affecting the activation variable $\alpha_{nKC}(V)$ similar to how we modelled use-dependent inactivation for I_{Ca} except $\alpha_n(V)$ increases with calcium.

We use a method similar to Chapter 4 of [35] by Yamada, Koch, and Adams. We have the following equation.

$$\alpha_{hKC}(V) = z(Ca)a_0 e^{\frac{-\delta V}{s}} \tag{4.40}$$

which can be rearranged so that as before the calcium dependence is in V_{nKC} giving

$$V_{n,new} = V_{n,old} + K_n \ln(z(Ca))$$

where

$$z(Ca) = 1 + \frac{ca1}{(1 + \exp^{((-Ca+ca2)/ca3)})}$$

and ca1, ca2 and ca3 are all constants fit from the data taken from Figure 2F of Zhang [36] which plots activation against calcium concentration. We rescaled the function so at the resting value of calcium z(Ca)=0. The simplified effect of this calcium dependence is an increase in calcium causes the $n_{KC\infty}(V)$ curve to shift to the left making the current activate at lower membrane potentials.

Discussion

The voltage clamp experiment from Figure 2A of Zhang [37] was simulated in Figure 4.15. The effect of the calcium level on I_{KC} can be seen in Figure 4.16. Due to the lack of data on internal levels of calcium we have some difficulty and need to adjust the parameters of the calcium dependence to increase the effect so that it is noticeable. I_{KC} is a smaller current that is overpowered by the other inward potassium currents such that it generally does not seem to have much of an effect on the shape of the action potential.

4.4.6 Calcium Dynamics

We based our calcium dynamics on the work by Canavier [1] discussed in Section 4.4.6 and Methods in Neuronal Modeling Chapter 6 [30]. For our purposes, only the amount of calcium just inside the membrane is relevant. Thus we have a model where the amount of calcium coming into the cell is determined by the amount of calcium current, and once inside the cell calcium is absorbed into cellular stores. We have the following differential equation to describe this behaviour

$$[Ca]' = -f_{Ca}\frac{I_{Ca}(V)}{volF} - \beta([Ca] - [Ca_{min}]) \tag{4.41}$$

where vol is the volume of cell just inside the membrane which we are dealing with, F is Faraday's constant, f_{Ca} is a weight constant which converts the amount of I_{Ca} into the amount of calcium in the cell. β is rate at which calcium is absorbed into the cytoplasm of the cell and $[Ca_{min}]$ is the minimum amount of calcium present in the outer layer of the membrane.
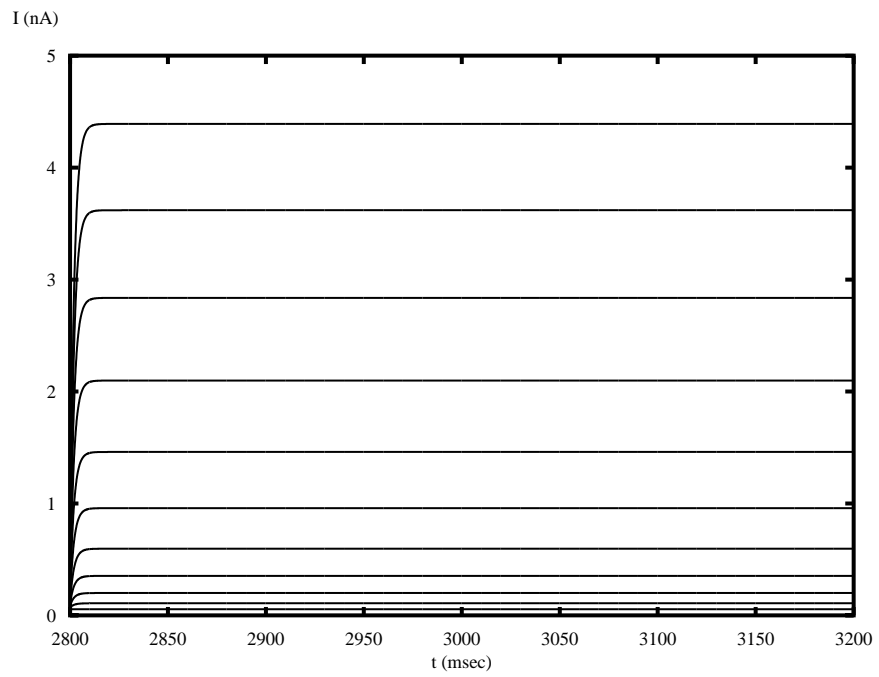
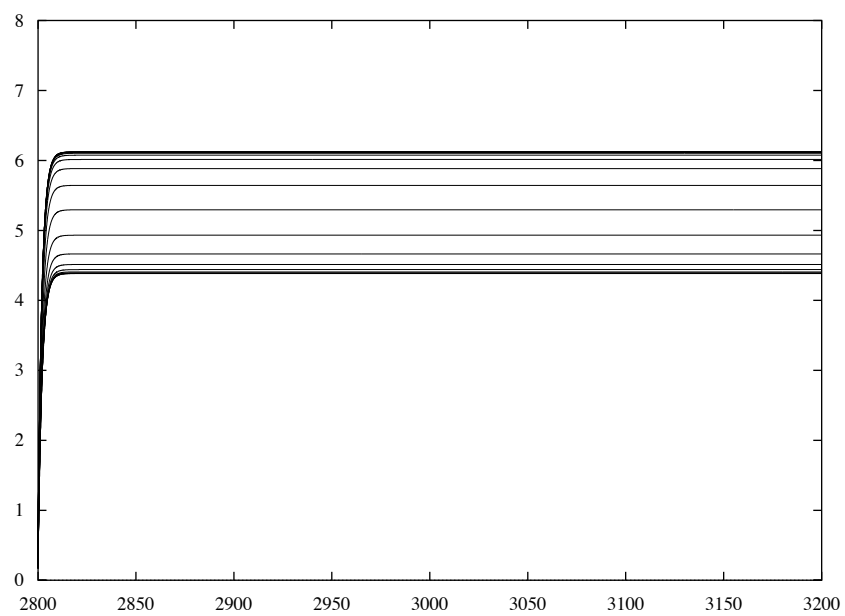Figure 4.15: Voltage Clamp for I_{KC}

Figure 4.16: I_{KC} Voltage Clamp with $V_{pre} = -60$ and $V = 40$ with calcium level ranging from 0 (bottom) to 20 (top) in steps of 1 mM

4.5   Action Potential

The action potential in an Aplysia bag-cell neuron is different from other neurons in that the action potential does not exhibit threshold behaviour. Most neurons have a threshold that if the input current pushes the membrane voltage above it, the ion channels in the cell cause a spike to occur. The spike does not depend on the strength of the input as long as the membrane potential the threshold. However in bag-cells the spiking behaviour seen in papers such as Magoski et al.[15] clearly shows the upstroke of the action potential to occur entirely while the stimulus current is on. As soon as the stimulus ceases the voltage rapidly returns to its resting state. In fact during a spike train where the cell is stimulated at 5Hz for 50 spikes, the voltage drops severely before the input has even stopped during the first spike and gradually drops less as the spike changes shape during the spike train. For a basic understanding of how the currents in the bag-cell neuron work together see all activation and inactivation steady state curves in Figure 4.17. These steady state curves are useful for describing when a given current is active at a glance. We found that the steady state of n_{K1} to cause a problem with the full model due to it being greater than 0 at very low voltages. This leads to the K1 current overpowering the upstroke of an action potential and thus we will start with a simpler version of the model.

First we will start by building a model containing just I_{Ca}, I_{K2} and I_L similar to the model made by Quattrocki et al. [27]. We found that the model parameters can be adjusted to give us a very good representation of an initial spike in a spike train shown in Magoski et al.'s 2007 paper [15]. A spike train is a method used to experimentally induce an afterdischarge in a bag-cell neuron. Using a sharp electrode current clamp the cell is forced to fire at 5 HZ for 10 seconds. The input is 1 nA for 50 ms then 150 ms off. After the spike train has finished the cell will enter the afterdischarge state within a few minutes. The action potential has a height of 80 to 90 mV and usually has returned to rest within 50 msec of the stimulus ending.

We found the model to be very sensitive to different parameters. Specifically when adjusting the maximum conductance for different currents there are two problems we encounter. If the calcium conductance is too low then when the initial stimulus is applied I_{Ca} will not be strong enough to overcome the potassium currents and we end up with a "spike" as seen in Figure 4.18. However when I_{Ca} is strong enough for the spike to reach the correct height, a second steady state appears if there is not the right amount of potassium current to bring the spike downwards. An example of this can be seen in Figure 4.19. If we correctly set up the balance between I_{K2} and I_{Ca} we can create a spike almost identical to the first spike of the spike train seen in Magoski et al. [15] both qualitatively and quantitatively.

We then add in the remaining currents, I_{KC} and I_A, as well as the calcium dynamics and use-dependent inactivation for I_{Ca}. The calcium dynamics parameters needed to be adjusted so in order to fit with the larger calcium conductance we required to get proper spiking behaviour. We also found that if we increase the activation time constant of I_{K2} slightly and decrease the inactivation time constant of I_{Ca} we can cause the spike behaviour
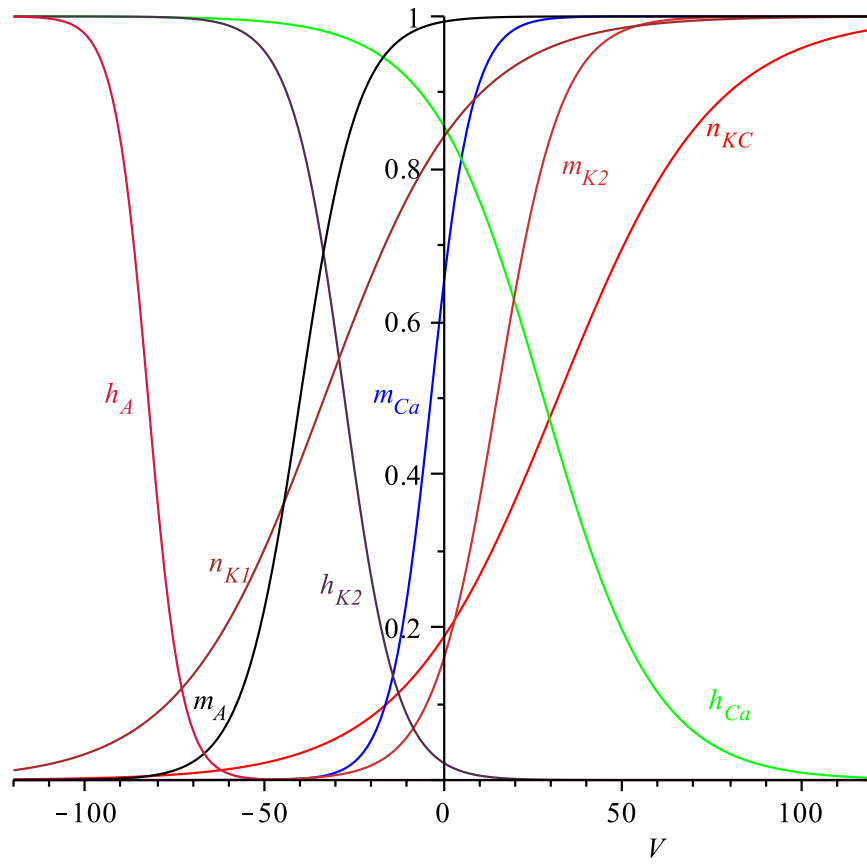
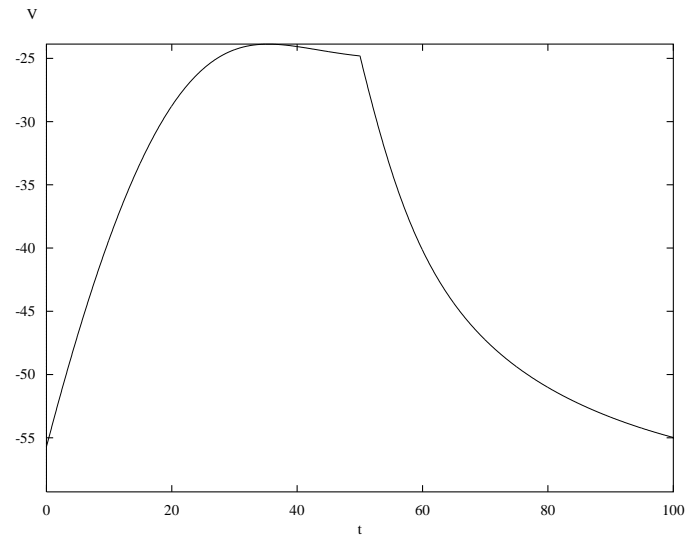Figure 4.17: Activation and Inactivation Steady State Curves

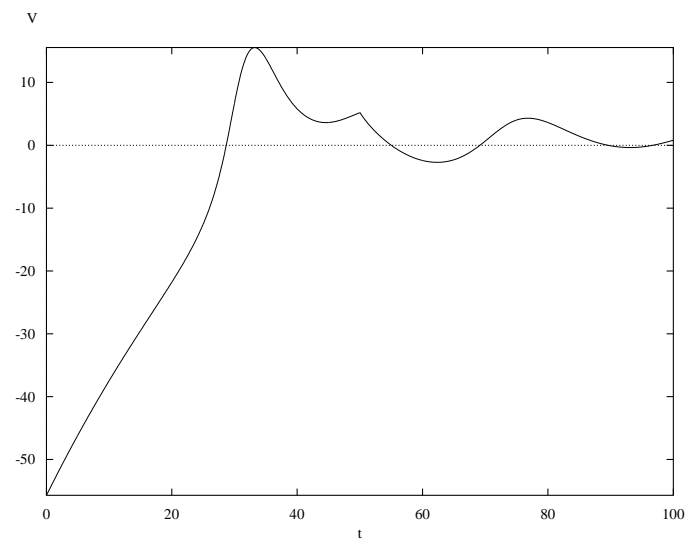Figure 4.18: Spike with Too Much Potassium Current

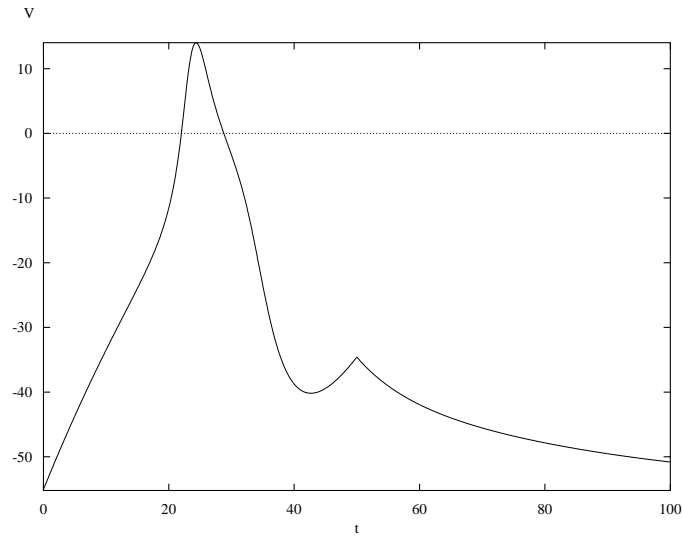Figure 4.19: Spike with not Enough Potassium Current

58

Figure 4.20: Spike using I_{Ca} and I_{K2} and Leak

where the membrane potential has started to drop before the stimulating current has been turned off. We simulated a spike train as seen in figures 1 and 4 of Magoski's 2007 paper [15]. The results are shown in Figure 4.21. We still do not include I_{K1} because even at very small conductance values it will significantly affect the spiking behaviour by overpowering the calcium current.

Figure 4.21 is a good representation of the spike train behaviour seen in Figure 4 of [15]. However the conductances we used to achieve the spike broadening were fairly large and relied mostly on the use-dependent calcium current inactivation for spike broadening. We have also not implemented any components within the model that will fundamentally change the cell's electrophysical properties so that it will spike spontaneously. In the next section we will introduce a few of the cAMP and PKC dependent mechanisms into our model to try and more accurately reproduce the spike broadening behaviour.

4.6 Further Work

4.6.1 PKC Activated Calcium Current

We implemented a basic version of a covert calcium channel which is physiologically activated by PKC, which in turn is activated by increased levels of cAMP. Using Strong et al.'s 1985 [4] letter to Nature which investigated the effect of a cAMP analogue on voltage clamp recordings of the calcium currents. We determined the activation variable properties for the
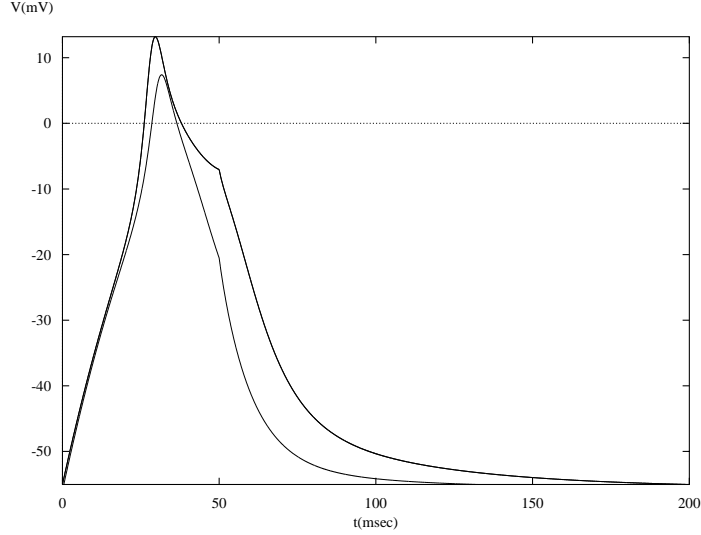
59

Figure 4.21: 1st and 50th Spike in Spike train of 5Hz

covert calcium channel which we denote as I_{PKC}. We chose to model I_{PKC} as an addition to the activation of the calcium current as follows

$$I_{Ca} = \bar{g}_{Ca}(m_{Ca}(V) + m_{PKC}(V))h_{Ca}(V)(V - E_{Ca}) \tag{4.42}$$

Where we determined data for $m_{\infty,PKC}(V)$ by subtracting Figure 2a from Figure 2b of [4] and using the same method as before which gives us the difference between the calcium current with and without the PKC activated component. The results are shown in Table 4.11 and Figure 4.22.

Table 4.11: I_{PKC} Parameter Fit Values

V_{mPKC}	K_{mPKC}	error
-5.0924	11	0.0074

However we need a mechanism to gradually turn the PKC activated current on so that it does not unbalance the dynamics of the system and cause the high steady state behaviour seen in Figure 4.18 which occurs whenever the ratio between calcium conductance and potassium conductance is too high. We chose to do this by multiplying $m_{PKC}(V)$ by the following

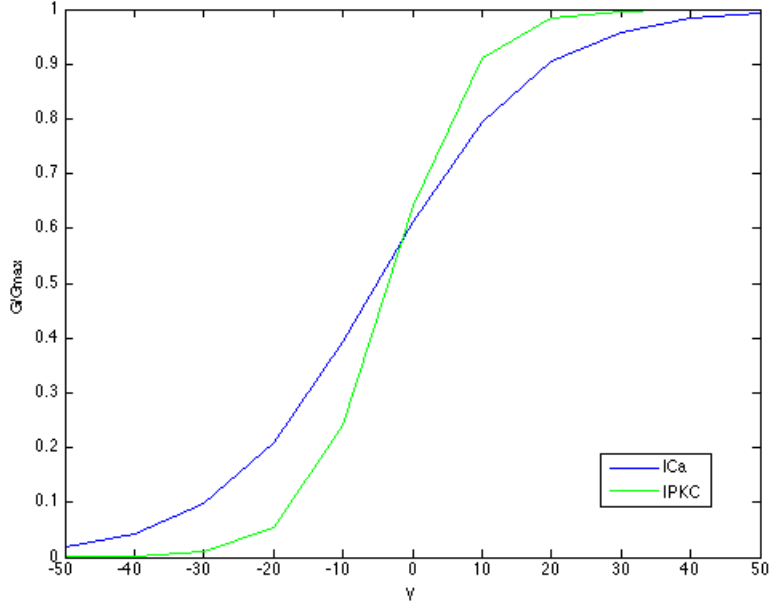$$f_{PKC}\frac{Ca}{Ca + C_{PKC}} \tag{4.43}$$

60

Figure 4.22: $m_{\infty PKC}(V)$ and $m_{\infty Ca}(V)$

where C_{PKC} is the calcium threshold for the activation of the PKC current and f_{PKC} is the fraction of additional calcium conductance contributed by the covert calcium channels.

$$I_{Ca} = \bar{g}_{Ca}(m_{Ca}(V) + f_{PKC}\frac{Ca}{Ca + C_{PKC}}m_{PKC}(V))h_{Ca}(V)(V - E_{Ca}) \qquad (4.44)$$

Also we have assumed that the PKC current is quite similar to the calcium current and thus assumed the same time constants and inactivation variable. We did this because of the limitations of the data we had and because the increase in calcium conductance from this channel is a component in causing spike broadening. In the future we would want an equation of the form

$$I_{PKC} = \bar{g}_{PKC}(PKC)m_{PKC}(V)h_{PKC}(V)(V - E_{Ca}) \qquad (4.45)$$

where the maximal conductance is dependent on the amount of PKC available. If the timing aspects of the PKC current are significantly different from the normal calcium current then the PKC could be one of the most important components of causing an afterdischarge.

4.6.2   cAMP Dependent K2 Inactivation

In order to improve the spike broadening aspect of our model, we want to introduce the cAMP-dependent inactivation of I_{K2} mentioned in Section 3.3 which was originally inves-

61

tigated by Strong[32]. Since we have not implemented cAMP dynamics, we use calcium to represent the amount of cAMP since during a spiking both calcium and cAMP levels increase. Similar to our modulation of the PKC current we multiplied both g_{K2} and τ_{hK2} by a function of the form

$$1 + \frac{C_{K2}}{C_{K2} + Ca} \tag{4.46}$$

where C_{K2} is a constant that may have a different value for g_{K2} and τ_{hK2}, however when fitting the parameters to simulate the correct behaviour we found the same value for both gave us the amount of spike broadening we wanted. In order to implement this we had to decrease the value of g_{K2} and τ_{hK2} since the value of our calcium dependent function is always greater than 1. The results of using these changes in addition to the PKC current can be seen in Figure 4.23 and the full spike train and the resulting changes in calcium levels can be seen in Figure 4.24. The spikes do represent the experimental data quite well although there a few flaws. The peak for the 50th spike should be shifted a little more to the right and the initial downstroke before the stimulus is turned off is more curved than it should be. We also overshoot the resting potential during hyperpolarization which does not seem to occur during experimental spikes. A lot of the inconsistencies between the experimental spike and simulated spike seem to be due to the fact we did not have enough data to accurately model the time constant functions over a sufficient range of membrane potential. The time constant parameters are generally the most important parameters for adjusting the spike behaviour in our model.

4.6.3   Prolonged Depolarizing Current

Magoski's 2007 paper [15] described a prolonged depolarizing current that occurs after the spike train leading up to the afterdischarge behaviour that could help explain the change in electrophysical properties which causes a cell which does not have a normal spike to spike spontaneously. The current is thought to be a nonselective cation current which activates due to the influx of calcium during the spike train.

The calcium is thought to activate the depolarizing current by first activating the protein calmodulin which in turn activates the nonspecific cation channel. Magoski et al. consider that there may be a window where the correct level of calcium activates this current during the spike train. For our purposes of trying to achieve the resulting membrane potential behaviour, we can simply have the channel activate at a specific time when a certain level of calcium is reached at the end of the spike train. The current typically raises the membrane potential from -60 mV to -45 mV over 20-30 seconds and lasts for 3-5 minutes. The current can be modelled by an equation of the form
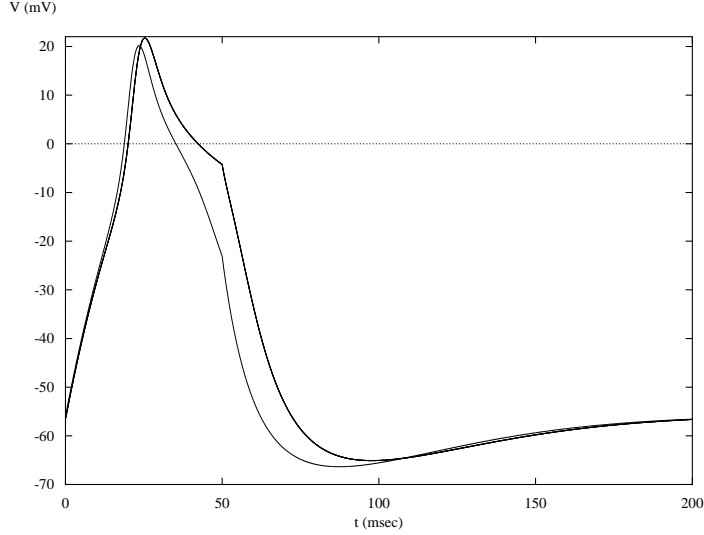
$$I_{PD} = \bar{g}_{PD} m_{PD} (V - E_{PD}) \tag{4.47}$$

Figure 4.23: 1st (narrower) and 50th (wider) Spike in Spike train of 5 Hz with additional PKC and K2 inactivation

where

$$\frac{\mathrm{d}m_{PD}}{\mathrm{d}t} = \frac{m_{PD\infty}(t) - m_{PD}}{\tau_{mPD}} \tag{4.48}$$

and

$$m_{PD\infty} = H(t - t_{PD}) \tag{4.49}$$

where we simply model the activation variable using a Heaviside function for now where the inactivation variable switches from 0 to 1 when peak level of calcium is reached at the end of the spike train, t_{PD}.

The three remaining parameters for this channel can be easily fit by eye by running a simulation with no stimulating current and adjusting the parameters until the proper behaviour is observed. The parameters $\bar{g}_{PD}$ and E_{PD} can be adjusted to determine the new resting potential with I_{PD} turned on and τ_{mPD} can be used to adjust the speed at which the membrane potential approaches the new steady state. We have incorporated this into our model in Figure 4.25 by running the simulation using two different time steps, 0.05 msec for the spike train and 1 msec afterwards. The full model with all parameter values can be seen in the Appendix.
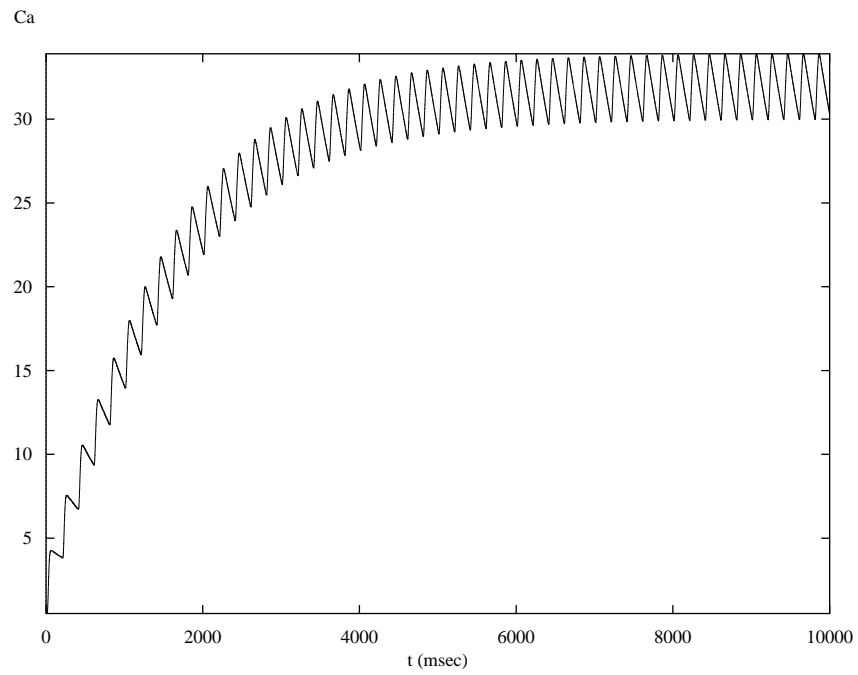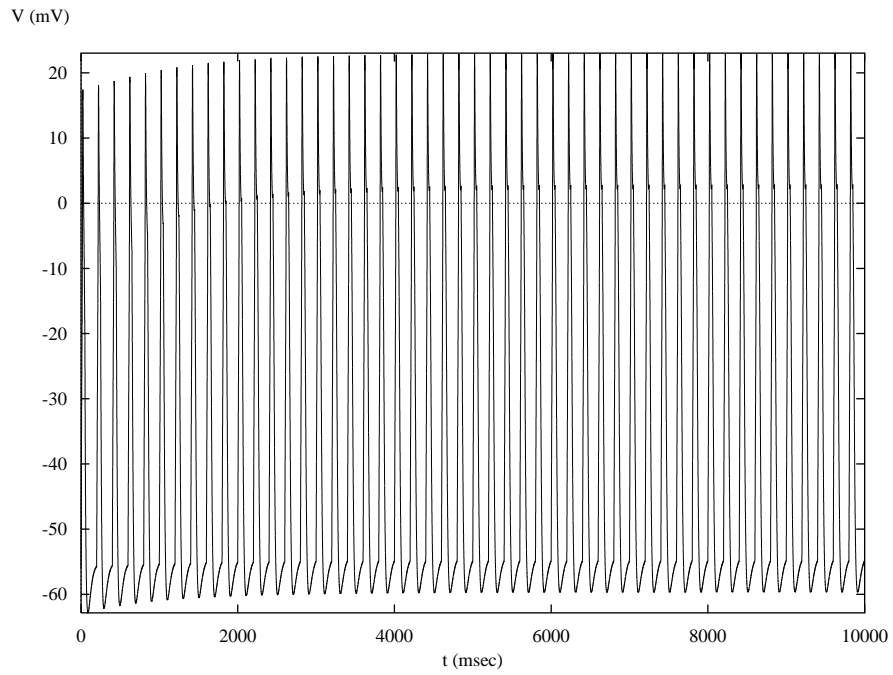
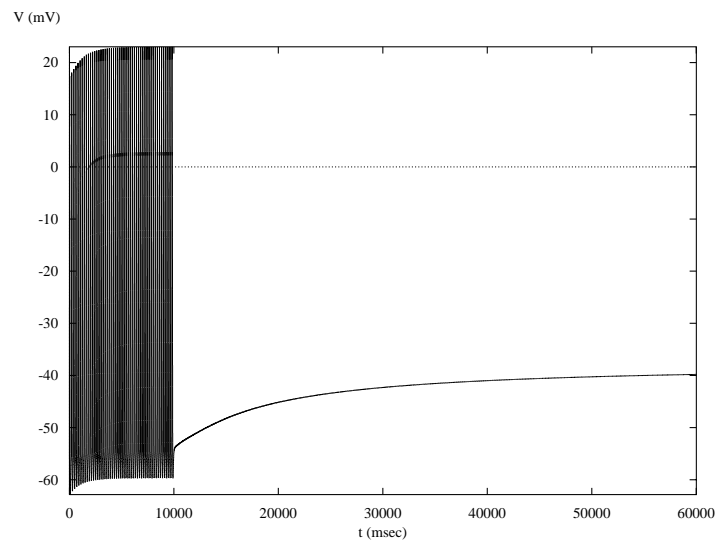Figure 4.24: Spike Train and Calcium Activity During Spike Train, Each Spike in Calcium Occurs Over 200 ms

64

Figure 4.25: Spike Train with Prolonged Depolarizing Current

65

Chapter 5

Conclusion

The Aplysia and its bag-cell neuron has been an important object of study for neuroscientists over the last 40 years. Due to the relative simplicity of the Aplysia's central nervous system it is possible to understand the effects of a specific type neuron on the overall behaviour of the animal. The bag-cell neuron is known to release a hormone that causes the onset of a series of behaviours culminating in the animal laying eggs. The specific mechanism through which this occurs is known as an afterdischarge. The bag-cell neurons will fire synchronously for approximately 20 minutes releasing the egg laying hormone into circulation. Half an hour after the afterdischarge the egg laying behaviour will begin. In vitro an afterdischarge is stimulated by stimulating the cell repeatedly at 5 Hz for 1 second, which is followed by a short delay and then the after discharge behaviour occurs.

The resting bag-cell neuron exhibits six main currents: I_{Ca}, I_{K1}, I_{K2}, I_A, I_{KC} and I_L. I_{Ca} is a voltage-gated calcium channel that is responsible for the upstroke of the action potential and exhibits use-dependent inactivation. I_{K1} and I_{K2} are voltage gated potassium channel responsible for hyperpolization during an action potential as well as spike broadening. I_A is a voltage gated potassium channel responsible for membrane potential behaviour at very negative values. I_{KC} is a voltage and calcium dependent potassium channel that affects spike broadening and cell excitability. I_L is the leak current and is a non specific cation channel that determines the resting potential of a cell. Using voltage clamp experiments by Strong, Kaczmarek, and Magoski we were able to fit equations that describe the behaviour of the different ion channels. The equations were based on the Nobel prize winning work of Hodgkin and Huxley described in Section 2.3. We were able to create a model that represented very well the spiking behaviour of a bag-cell neuron when stimulated although we had to remove the I_{K1} current to do so. The model still needs more work to be able to describe the afterdischarge behaviour. There is a fundamental change in the electrophysiology that occurs during the spike train stimulus that causes the cell to go from non-excitable to spontaneous firing. The possible factors that cause this shift are described in the next section.

5.1 Future Work

5.1.1 cAMP Dependence

From Strong and Kaczmarek's papers ([4],[32],[2]), evidence suggests that cyclic adenosine monophosphate (cAMP) plays a key role in modulating the conductances of the ion channels of an Aplysia bag-cell neuron to cause afterdischarge behaviour. Bag-cell neurons also contain a cAMP dependent protein kinase which affects certain types of potassium currents, see ([15], [2]). The outward potassium currents are generally reduced in overall conductance and also exhibit a decreased inactivation time due to cAMP, whereas PKC acts to increase the calcium conductance by activating covert calcium channels. Injecting cAMP analogues into bag-cells has been shown to induce afterdischarge behaviour.

5.1.2 Electrical Coupling

Aplysia bag-cell neurons are found in two clusters of several hundred neurons which are electrically coupled. As previously discussed, bag-cells are coupled by a gap junction which is when two cells are so close together that ions freely flow from cell to another. Afterdischarge behaviour does not require the gap junctions to work however it does help synchronize the behaviour of multiple cells. To model electrical coupling we will use the example from Rinzel's 1991 paper [29] which modelled synchronization of pancreatic β cells. The governing equation was modified to include a term representing the flow of charge between different neurons through gap junctions. The cells were assumed to be homogeneous and the current flowing through the gap junction was assumed to equalize the membrane potentials, i.e. if cell j hyperpolarizes cell k then cell k depolarizes cell j. The governing equation for the jth neuron is as follows:

$$C\frac{dV_j}{dt} = -\sum I_{ion} - \bar{g}_c \sum_{k \in \Omega_j} (V_j - V_k) \tag{5.1}$$

where $\bar{g}_c$ is the conductance of the gap junction current and we sum over all the cells which neuron j is connected to, Ω_j.

5.1.3 Afterdischarge Discussion

In order to elicit afterdischarge behaviour there are several possibilities. The first and least likely but easiest to implement is that during the spike train the increased levels of cAMP cause a new current to slowly switch on which has the effect of constantly stimulating the cell and causing it to spike.

The current research, however, suggests that the effects of cAMP and PKC change the dynamical system so that it spontaneously fires. However it is hard to determine exactly how

this may occur given that all the data taken from voltage and current clamp experiments suggest the cell does not actually have a proper action potential even when stimulated. The most significant cause of this behaviour seems to be the covert calcium current. Unlike many other neurons, the bag-cell lacks any sodium current which is generally responsible for the upstroke behaviour in action potentials. If the calcium current changes the dynamics of the system so that it now exhibits threshold behaviour then it is possible the effects of cAMP on the inward potassium currents create a low enough threshold that the prolonged depolarizing current pushes the membrane potential above the threshold for the duration of the afterdischarge.

Appendix: Model Details

Units: millivolts, milliseconds, nanoamps, microsiemens, nanofarads

Initial Conditions

$$V = -56$$
$$n_{K1} = 0.2$$
$$m_{K2} = 0$$
$$h_{K2} = 1$$
$$m_{Ca} = 0$$
$$h_{Ca} = 1$$
$$ca = .5$$
$$m_A = 0.1$$
$$h_A = 0$$
$$m_{PD} = 0$$
$$m_{PKC} = 0$$

Capacitance

$$C_m = .5$$

Nernst Potentials

$$E_k = -80$$
$$E_{Ca} = 57.599$$

I_{K1} **Parameters**

$$g_{K1} = 0$$
$$V_{nK1} = -31.4888$$
$$K_{nK1} = 18.7711$$
$$p_{nK1} = 1$$
$$\tau_{nK1} = 5$$

I_{K2} **Parameters**

$$g_{K2} = 0.2$$
$$V_{mK2} = 10$$
$$K_{mK2} = 8.9335$$
$$p_{mK2} = 1$$
$$\tau_{0mK2} = 9$$
$$C_{K2\tau} = 50$$
$$C_{K2g} = 50$$
$$K_{hK2} = 7$$
$$\tau_{0hK2} = 88.7305$$

I_{Ca} **Parameters**

$$g_{Ca} = 0.15$$
$$V_{mCa} = -3.3863$$
$$K_{mCa} = -5.7564$$
$$p_{mCa} = 1$$
$$\tau_{0mCa} = 8.5338$$
$$\delta_{mCa} = .6586$$
$$Kca = 600$$
$$V_{hCa}0 = -11.69$$
$$K_{hCa}0 = 7.5$$
$$\tau_{0hCa} = 70$$

I_{PKC} **Parameters**

$$fracPKC = 0.2$$
$$V_{mPKC} = -5.0924$$
$$K_{mPKC} = 11.2011$$
$$p_{mPKC} = 1$$
$$C_{PKCCa} = 30$$

I_{KC} **Parameters**

$$g_{KC} = 0.0588$$
$$V_{nKC}0 = 28.5737$$
$$K_{nKC}0 = -23.0909$$
$$p_{nKC} = 1$$
$$\tau_{0nKC} = 2$$

I_L **Parameters**

$$g_L = 0.01$$
$$V_L = -55$$

Calcium Parameters

$$f_{Ca} = .3$$
$$vol = 6.5449847e - 11$$
$$Ca_{min} = 0.3$$
$$\beta = 0.3$$
$$Fconst = 96487e6$$

I_{KC} **Calcium Fit Parameters**

$$Ca1 = 1.4469$$
$$Ca2 = 10.096$$
$$Ca3 = 1.1477$$

I_A **Parameters**

$$g_A = 0.36$$
$$V_{mA} = -39.9174$$
$$K_{mA} = 8.0696$$
$$p_{mA} = 1$$
$$\tau_{0mA} = 22.7511$$
$$\delta_{mA} = .2272$$
$$V_{hA} = -82.4$$
$$K_{hA} = -4.7$$
$$\tau_{0hA} = 250$$

Stimulating Current Parameters

$$I_{stim} = 1.2$$
$$t_{stim} = 50$$

Stimulating Current Equation

$$I_{pulse} = I_{stim}(heav(t) - heav(t - t_{stim}))$$

Governing Equation

$$V' = -(I_A + I_{K1} + I_{K2}(V) + I_{Ca} + I_L(V) - I_{pulse})/C_m$$

I_{K1} Equations

$$n_{K1\infty}(V) = (1 + exp(-(V - Vn_{K1})/Kn_{K1}))^{-p_{nK1}}$$
$$n'_{K1} = (n_{K1\infty}(V) - n_{K1})/\tau_{nK1}$$
$$I_{K1}(V) = g_{K1}n_{K1}(V - E_K)$$

I_{K2} Equations

$$m_{K2\infty}(V) = (1 + exp(-(V - V_{mK2})/K_{mK2}))^{-p_{mK2}}$$
$$m'_{K2} = (m_{K2\infty}(V) - m_{K2})/\tau_{0mK2}$$
$$h_{K2\infty}(V) = (1 + exp((V - V_{hK2})/K_{hK2}))^{-1}$$
$$h'_{K2} = (h_{K2\infty}(V) - h_{K2})/(\tau_{0hK2} * (1 + C_{K2\tau}/(C_{K2\tau} + Ca)))$$
$$I_{K2}(V) = g_{K2}(1 + C_{K2g}/(C_{K2g} + Ca)))m_{K2}h_{K2}(V - E_K)$$

I_{Ca} Equations

$$m_{Ca\infty}(V) = (1 + exp((V - V_{mCa})/K_{mCa}))^{-p_{mCa}}$$
$$m_{PKC\infty}(V) = (1 + exp((V - V_{mPKC})/K_{mPKC}))^{-1}$$
$$\tau_{mCa}(V) = 3.3308exp(-V/83.256)$$
$$v_{hCa}(Ca) = V_{hCa0} + (K_{hCa0}ln(1 + 1/(Ca - 0.3)))$$
$$h_{Ca\infty}(V) = (1 + exp((V - V_{hCa}(Ca))/K_{hCa0}))^{-1}$$
$$\tau_{hCa} = \tau_{0hCa}$$
$$m'_{Ca} = (m_{Ca\infty}(V) - m_{Ca})/\tau_{mCa}(V)$$
$$h'_{Ca} = (h_{Ca\infty}(V) - h_{Ca})/\tau_{hCa}$$
$$I_{Ca}(V) = g_{Ca}(m_{Ca} + fracPKC * (Ca/(Ca + C_{PKCg})) * m_{PKC})h_{Ca}(V - E_{Ca})$$

I_{KC} Equations

$$z(ca) = 1 + ca1/(1 + exp((-ca + ca2)/ca3))$$
$$V_{nKC}(Ca) = V_{nKC0} + (K_{nKC0}ln(z(ca)))$$
$$n_{KC\infty}(V) = (1 + exp((V - Vn_{KC}(Ca))/Kn_{KC0}))^{-p_{nKC}}$$
$$\tau_{nKC} = \tau_{0nKC}$$
$$n'_{KC} = (n_{KC\infty}(V) - n_{KC})/\tau_{nKC}$$
$$I_{KC}(V) = g_{KC}n_{KC}(V - E_K)$$

I_A Equations

$$m_{A\infty}(V) = (1 + exp(-(V - V_{mA})/K_{mA}))^{-p_{mA}}$$
$$\tau_{mA}(V) = \tau_{0mA}exp(\delta_{mA}(V - V_{mA})/K_{mA})/(1 + exp((V - V_{mA})/K_{mA}))$$
$$h_{A\infty}(V) = (1 + exp(-(V - V_{hA})/K_{hA}))^{-1}$$
$$\tau_{hA} = \tau_{0hA}$$
$$m'_A = (m_{A\infty}(V) - m_A)/\tau_{mA}(V)$$
$$h'_A = (h_{A\infty}(V) - h_A)/\tau_{hA}$$
$$I_A(V) = g_A m_A h_A(V - E_K)$$

Leak Current Equation

$$I_L(V) = g_L(V - V_L)$$

Calcium Dynamics Equation

$$Ca' = -f_{Ca}I_{Ca}(m_{Ca}, h_{Ca}, V)/(volFconst) - \beta(Ca - CaMin)$$

References

[1] C. C. Canavier, J. W. Clark, and J. H. Byrne. Simulation of the bursting activity of neuron R15 in *Aplysia* : Role of ionic currents, calcium balance, and modulatory transmitters. *Journal of Neurophysiology*, 66(6):2107–2124, December 1991. 26, 53

[2] P. J. Conn and L. K. Kaczmarek. The bag cell neurons of *Aplysia*. *Molecular Neurobiology*, 3:237–273, 1989. 19, 67

[3] P. J. Conn, J. A. Strong, and L. K. Kaczmarek. Inhibitors of protein kinase c prevent enhancement of calcium current and action potentials in peptidergic neurons of *Aplysia*. *The Journal of Neuroscience*, 9(2):480–487, 1989. 23

[4] S. A. DeRiemer, J. A. Strong, K. A. Albert, P. Greengard, and L. K. Kaczmarek. Enhancement of calcium current in *Aplysia* neurones by phorbol ester and protein kinase c. *Nature*, 313:313–316, 1985. 59, 60, 67

[5] G. B. Ermentrout and D. H. Terman. *Mathematical Foundations of Neuroscience*. Springer, 2010.

[6] T. E. Fisher, S. Levy, and L. K. Kaczmarek. Transient changes in intracellular calcium associated with a prolonged increase in excitability in neurons of *Aplysia* californica. *Journal of Neurophysiology*, 71(3):1254–1257, March 1994.

[7] W.T. Frazier, E. R. Kandel, I. Kupfermann, R. Waziri, and R. E. Coggeshall. Morphological and functional properties of identified neurons in the abdominal morphological and functional properties of identified neurons in the abdominal ganglion of *Aplysia* californica. pages 1288–1351, 1967.

[8] K. E. Gardam, J. E. Geiger, C. M. Hickey, A. Y. Hung, and N. S. Magoski. Flufenamic acid affects multiple current and causes intracelular ca^{2+} release in *Aplysia* bag cell neurons. *Journal of Neurophysiology*, 2008. 47

[9] B. Hille. *Ion Channels of Excitable Membranes 3rd Edition*. Sinauer Associates, Inc., 2001. 8

[10] A. Hodgkin and A. Huxley. The components of membrane conductance in the giant axon of *Loligo*. *J. Physiol.*, (116):473–496, 1952. 11

[11] A. Hodgkin and A. Huxley. Currents carried by sodium and potassium ions through the membrane of the giant axon of *Loligo*. *J. Physiol.*, (116):449–472, 1952. 11, 12

[12] A. Hodgkin and A. Huxley. The dual effect of membrane potential on sodium conductance in the giant axon of *Loligo*. *J. Physiol.*, (116):197–506, 1952. 11

[13] A. Hodgkin and A. Huxley. A quantative description of membrane current and its application to conduction and excitation in nerve. *J. Physiol.*, (117):500–544, 1952. 11

[14] A. Hodgkin, A. Huxley, and B. Katz. Measurement of current-voltage relations in the membrane of the giant axon of *Loligo*. *J. Physiol.*, (116):424–448, 1952. 9, 11

[15] A. Y. Hung and N. S. Magoski. Activity-dependent initiation of a prolonged depolarization in *Aplysia* bag cell neurons: Role for a cation channel. *J Neurophysiol*, 97(3):2465–2479, 2007. 24, 49, 50, 51, 56, 59, 62, 67

[16] L. K. Kaczmarek, K. Jennings, and F. Strumwasser. Neurotransmitter modulation, phosphodiesterase inhibitor effects, and cyclicamp correlates of afterdischarge in peptidergic neurites. *Proceeding of the National Academy of Sciences of the United States of America*, 75(10):5200–5204, October 1978. 22

[17] L. K. Kaczmarek and J. A. Kauer. Calcium entry causes prolonged refractory period in peptidergic neurons of *Aplysia*. *The Journal of Neuroscience*, 3(11):2230–2239, 1983. 22

[18] L. K. Kaczmarek and F. Strumwasser. A voltage clamp analysis of currents underlying cyclic amp-induced membrane modulation in isolated peptidergic neurons of *Aplysia*. *Journal of Neurophysiology*, 52(2):30–349, 1984.

[19] J. Keener and J. Sneyd. *Mathematical Physiology*. Springer, 1998. 8

[20] C. Koch. *Biophysics of Computation: Information Processing in Single Neurons*. Oxford University Press, 1999. 15

[21] I. Kupfermann. Stimulation of egg laying by extracts of neuroendocrine cells (bag cells) of abdominal ganglion of *Aplysia*. *Journal of Neurophysiology*, 33(6):877–881, 1970. 21

[22] I. Kupfermann and E. R. Kandel. Electrophysiological properties and functional interconnections of two symmetrical neurosecretory clusters (bag cells) in abdominal ganglion of *Aplysia*. *Journal of Neurophysiology*, 33(6):867–876, 1970. 21

[23] A. Lee and W. A. Catterall. ca^{2+}-dependent modulation of voltage-gated ca^{2+} channels. In G. Zamponi, editor, *Voltage-Gated Calcium Channels*, chapter 11, pages 183–193. Landes Bioscience/ Eurekah.com, 2005. 49

[24] G. Marmont. Studies on the axon membrane. *J Cell Physiol.*, 34(3):351–382, 1949. 9

[25] E. Neher and B. Sakmann. Single-channel currents recorded from membrane from membrane of denervated frog muscle fibres. *Nature*, 260:779–802, 1976. 11

[26] T. A. Nick, L. K. Kaczmarek, and T. J. Carew. Ionic currents underlying developmental regulation of repetitice firing in *Aplysia* bag cell neurons. *The Journal of Neuroscience*, (16):7583–7598, 1996.

[27] E. A. Quattrocki, J. Marshall, and L. K. Kaczmarek. A shab potassium channel contributes to action potential broadening in peptidergic neurons. *Neuron*, 12:73–86, January 1994. 23, 24, 25, 39, 41, 56

[28] J. Rinzel. Discussion: Electrical excitability of cells, theory and experiment: Review of the hodkin-huxley foundation and update. *Bulletin of Mathematical Biology*, 52(1/2):5–23, 1990.

[29] J. Rinzel and A. Sherman. Model for synchronization of pancreatic β-cells by gap junction coupling. *Biophysical Journal*, 59:541–599, March 1991. 67

[30] E. De Schutter and P. Smolen. Calcium dynamics in large neuronal models. In C. Koch and I. Segev, editors, *Methods in Nueronal Modeling: From Ions to Networks*, chapter 6, pages 211–250. MIT Press, 2nd edition, 1998. 53

[31] J. A. Strong. Modulation of potassium current kinetics in bag cell neurons of *Aplysia* by an activator of adenylate cyclase. *The Journal of Neuroscience*, 4(11):2772–2783, 1984. 22, 36, 39

[32] J. A. Strong and L. K. Kaczmarek. Multiple components of delayed potassium current in peptidergic neurons of *Aplysia*: Modulation by an activator of adenylate cyclase. *The Journal of Neuroscience*, 6(3):814–822, March 1986. 22, 62, 67

[33] F. Strumwasser, L. K. Kaczmarek, and K. Jennings. Intracellular modulation of membrane channels by cyclic amp-mediated protein phosphorylation in peptidergic neurons of *Aplysia*. *Fed Proc.*, 41(13):2933–2939, 1982. 22

[34] A. R. Willms, D. J. Baro, R. M. Harris-Warrick, and J. Guckenheimer. An improved parameter estimation method for Hodgkin-Huxley models. *Journal of Computational Neuroscience*, (6):144–168, 1999. 29, 50

[35] W. M. Yamada, C. Koch, and P. R. Adams. Multiple channels and calcium dynamics. In C. Koch and I. Segev, editors, *Methods in Nueronal Modeling: From Ions to Networks*, chapter 4, pages 137–170. MIT Press, 2nd edition, 1998. 53

[36] Y. Zhang, W. J. Joiner, A. Bhattacharjee, F. Rassendren, N. S. Magoski, and L. K. Kaczmarek. The appearance of a protein kinase a-regulated splice isoform of slo is associated with the maturation of neurons that control reproductive behavior. *The Journal of Biological Chemistry*, 279(50):52324–52330, December 2004. 23, 52, 53

[37] Y. Zhang, N. S. Magoski, and L. K. Kaczmarek. Prolonged activation of ca^{2+}-activated k^+ current contributes to the long-lasting refractory period of *Aplysia* bag cell neurons. *The Journal of Neuroscience*, 22(23):10134–10141, December 2002. 23, 47, 52, 53